行政院國家科學委員會專題研究計畫成果報告

利用脈動式電滲透流以提高溶質的質傳與分離速率

計畫類別：☑個別型計畫　　□整合型計畫
計畫編號：NSC92-2212-E-002-049
執行期間：92年8月1日至93年7月31日

計畫主持人：賴君亮

本成果報告包括以下應繳交之附件：
- □赴國外出差或研習心得報告一份
- □赴大陸地區出差或研習心得報告一份
- □出席國際學術會議心得報告及發表之論文各一份
- □國際合作研究計畫國外研究報告書一份

執行單位：國立台灣大學工學院機械工程學系

中華民國九十三年七月三十一日

摘　　要

隨著微機電技術日益地成熟，過去十年來微型化的趨勢與潛力受到科學家與工程師的重視，許多在傳統實驗室中需多個步驟分開的實驗，可以被濃縮在一微晶片中一次處理完成，因而可應用在化學反應實驗、不同物種的混合與分離、生物檢測、醫學臨床測試與環境控制等方面。架構在如此微小的尺寸上，本文探討在一注滿電解質與鈍性物種的微管中，當溶液受到一振盪式電滲透流驅動後，其鈍性物種的質傳與溶質分離的物理現象。

儘管過去五十年來，已經有許多研究探討微管表面的電雙層現象（EDL）、電滲透流的特性（EOF）以及泰勒傳遞現象（Taylor Dispersion）現象，然而本文所討論振盪式電滲透流與泰勒傳遞現象的結合則尚未有文獻發表，因此本研究不僅在晶片設計上具有參考價值，在學術上也具有相當地挑戰性與重要性。

文中複變函數被使用來計算出速度場、濃度場與質傳速率的解析解。結果顯示，質傳速率的增加會先隨無因次化頻率增加而後減少，這樣的變化與三個時間常數間的關係、以及統御方程式中的三個特徵值有關。此外，Schmidt 數、電雙層的厚度、雷諾數（Reynolds Number）、微管表面的電位、與外加電場的強度對質傳速率增加的影響，也都在本文中有系統地加以探討。

ABSTRACT

Over the last decade, the potential of micro-miniaturization of analytical procedures has been explored with the maturity of MEMS technology. Several sequential experiments steps are integrated into a single automated process. These microfluid chips can be applied to perform chemical reactions, mixing and separations, biological detections, medical testing, and environmental monitoring, etc. The present study is aimed at investigating theoretically the mass transfer and separation driven by an electroosmotic flow (EOF) in a micropipette.

Many researches about electrical double layer (EDL), EOF and Taylor dispersion have been published over the past five decades. However, the combination of a time periodic EOF and the phenomenon of Taylor dispersion is first investigated systematically in the present study.

A complex variable approach is used to solve analytically the solutions of the velocity profile, the concentration distribution, and the mass flow rate. The results show that the enhancement of mass transport rate, R_Q, arises first and then descends with the increase of the frequency of the electrical field applied. Parametric studies uncovered that three time constants, $t\omega \equiv \frac{1}{\omega}$, $t\nu \equiv \frac{r_0^2}{\nu}$, and $tD_n \equiv \frac{r_0^2}{D_n}$ together with the three eigenvalues in the governing equations Ω, ΩS_c, and K play significant roles in the process of mass transfer. The effects of Schmidt number, S_c, the thickness of EDL, K, Reynolds number, R_e, the electrical potential on the surface of the micropipette, Ψ_s, and the intensity of the applied electrical field, E_z^* on R_Q are systematically analyzed and discussed. It is also shown that at low frequency the oscillating EOF is conducive to the separation of species.

CONTENTS

CHAPTER 1

INTRODUCTION

1-1 Fundamental Physics

The development of lab-on-a-chip Microfluidics has been a major area of interest to the analytical community for some years already [1~5]. The enhancement of lab-on-a-chip technology makes the tests and experiments of chemical, biomedial, and environmental systems faster, more accurately, and cheaper. It is thus worthwhile to develop better approaches offered in these chips.

Here we analyze an electroosmostic flow (EOF) in microchannels which can be used in these chips. The relationships of EOF in a circular capillary tube as well as the mass transport of a neutral solved species and separation of two non-interactive neutral species in the tube are the focus of our research.

Before constructing the physical model, certain fundamental physics, e. g., electrical double layer (EDL), electroosmotic flow (EOF), and Taylor dispersion related to the present study will be briefly discussed first in the following.

Electrical Double Layer [6, 7, 8] **and Electroosmosis**

Generally, most substances will acquire surface electric charges when they are brought into contact with a polar medium. Some of the charging mechanism include ionization, ion adsorption, and ion dissolution. The surface charges influence the ion distribution in the polar medium, forming the electrical double layer (EDL). The formation of EDL is because some species in the polar medium may have preference for being near the surface. Ions of opposite charge (counter-ions) to that of the surface are attracted toward the surface while ions of like (co-ions) charge are repelled from the surface. The attraction and repulsion then leads to EDL. Therefore, the EDL means the separation of charges that occurs at the interface between two phases, and the EDL is viewed as the phenomenon of boundaries. And why it is called EDL is because it consists, ideally, of two regions of opposite charge.

There are many models and theories provided to describe EDL (See Appendix A). A more elaborate theory called Gouy-Chapman-Stern theory or Stern's theory is proposed by Stern in 1942 [6, 7]. It is the most used theory to explain the

phenomenon of EDL. Here we introduce it briefly. In Gouy-Chapman-Stern theory, shown in Fig. A.2-1, the problem is alleviated by dividing the charge into two regions: one is the compact or inner layer, and the other is the diffuse layer. The compact layer is very close to the wall, while The diffuse layer is further out from the wall where Poisson-Boltzmann equation (See Appendix B) may be expected. Because of the interactions of forces between molecules, ions in compact layer are strongly attracted to the wall and are immobile, but they are mobile in diffuse layer.

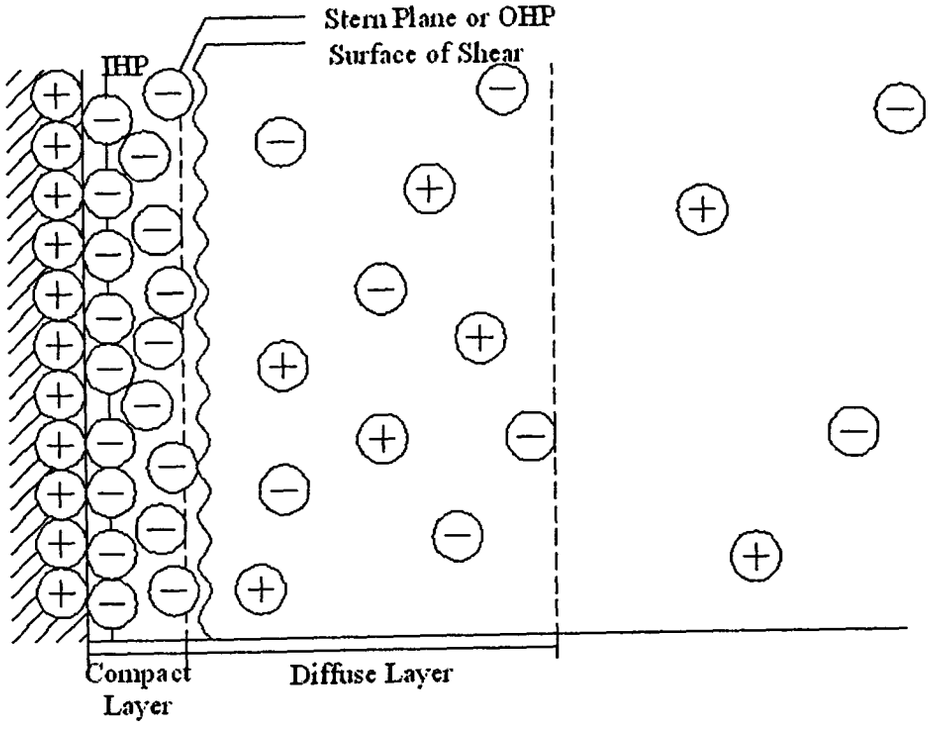

Fig. A.2-1 Structure of EDL established by Guoy-Chapman-Stern therory (After [6, 7])

Now an external tangential electric field is applied to electrical double layer. Inside EDL, the applied electric field can produce a small change in velocity over EDL, and thus a shear stress or velocity gradient at the surface can produce electrokinetic effects. That is, when mobile portion of the diffuse double layer and an external electric field interact in the viscous shear layer near the charged surface, the electrokinetic effects will arise. Helmbolta-Smoluchowski equation is the formula for the electroosmotic velocity past a plane charged surface. This is the most general theory to estimate the velocity at the "edge " of EDL and means it "slips" at the wall. (See Appendix A)

Electrokinetic effects contain four phenomena: electrophoresis, electroosmosis, streaming potential, and sedimentation potential. [7, 8] (See Appendix A). Here we

focus on the explanation of electroosmosis.

Electroosmosis describes the motion of fluids with respect to a stationary charged surface by an external electric field. When an electric filed is applied, an electrical body force is exerted on the excess counter-ions in the diffuse double layer of the EDL. The ions will move under the influence of the applied electric field, pulling the fluid with them. The fluid movement is carried through to the rest of the fluid by viscous force, resulting in an electroosmotic flow (EOF). [9, 10]

The phenomenon of EDL is usually neglected in macroscale fluid mechanics because the thickness of EDL ranges from a few nanometers up to several hundreds of nanometers. It is too thin to consider. However it can not be ignored in microscale systems. Due to the mobile ions in EDL under an applied electric field, the fluid will be driven. As a result, we use EOF as the driving force in our system.

Taylor Dispersion

G. I. Taylor [11~14] first analyzed the dispersion of one fluid injected into a circular capillary tube in which a second fluid was flowing. The two miscible liquids are contacted and mixed in a flow. So the miscible dispersion is called Taylor dispersion.

Taylor dispersion is caused by the coupling of diffusion and fluid flow. It can frequently be described by the same mathematics used so effectively for diffusion. However, they have much different physical origins. Here we illustrate the mechanism of Taylor dispersion.

But we should know the assumptions made in Taylor's experiment first:

The solutions are dilute.

The flow is laminar.

Mass transport is mainly by radial diffusion and axial convection. Other transport mechanisms are negligible.

As shown in Fig. 1.1-1 (Nunge & Gill,1969, when a patch of solute A is injected into a fully developed laminar flow of a solvent B at $t_0 = 0$), the dispersion of A into B takes place by pure axial molecular diffusion at very short time. This type of dispersion is very short and we have no interest in it.

As time is greater, $t_1 > 0$, axial convection starts to distort the solute patch into a parabolic shape because of the parabolic velocity field.

However, it is clear that axial convection establishes a radial concentration gradient. Thus at higher time, $t_2 > t_1$, radial molecular diffusion contributes to the dispersion process. At the front end of the patch, solute A in the center of the tube tends to toward the wall, thereby slowing the front end down. On the other hand, at the rear

end of the patch, solute A near the wall of the tube tends to diffuse toward the center simultaneously, thereby speeding the rear end up. The radial diffusion thus inhibits the dispersion induced by the axial convection. That is, the net effect of radial diffusion is to compress the mixing zone, which axial convection is to elongate. The result is therefore that there is a mixed zone of varying concentration.

As time goes on, $t_3 > t_2$, the mixed zone becomes more uniform. Finally at still larger time, t_4, a quasi-equilibrium is established. Here, convection, radial diffusion, and axial diffusion all contribute to the dispersion. With a further increase in time, the effect is only to increase the length of the mixed zone. Again, the type of dispersion is out of our interest.

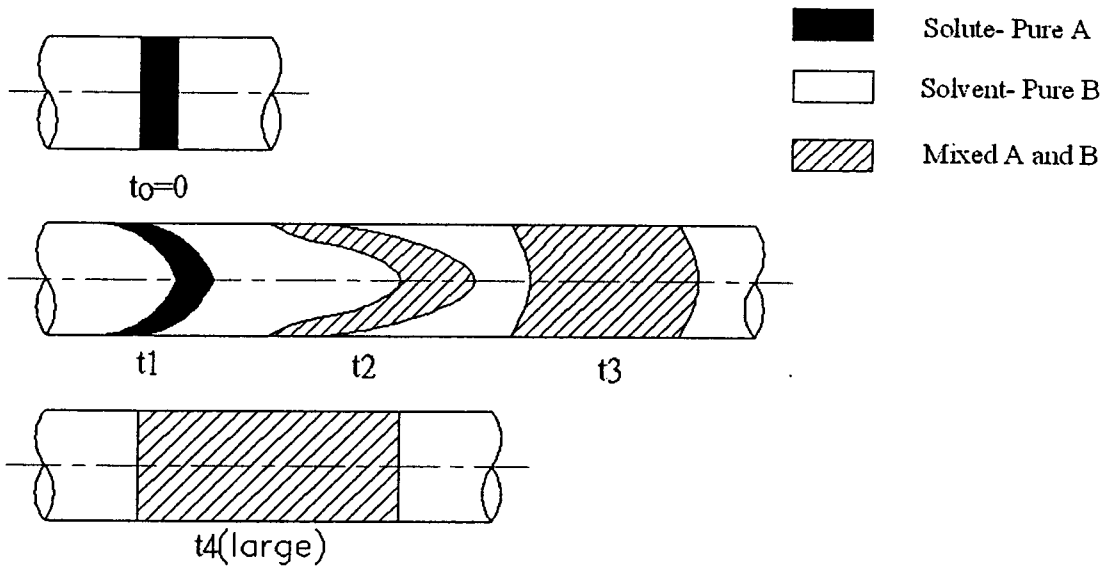

Fig. 1.1-1 Schematic of Taylor dispersion (after Nunge & Gill 1969)

The process of Taylor dispersion between t_1 and t_2 is much similar the mechanism of mass transport in our system. We then accept his points and use them to explain the mass transfer in the research.

1-2 Motivation and Objectives

Over the last decade, the potential of micro-miniaturization of analytical procedures has been explored with the maturity of MEMS and will play an important role on biochemical experiments. Several sequential experiments steps are integrated into a single automated process. This leads to the growth of the lab-on-a-chip technology. It means the entire laboratory is crammed on to a chip by the technology. These microfluid chips can be applied to perform chemical reactions, mixing and separations [15, 16, 17], biological detections, medical testing, and environmental monitoring, etc. Because of the micro-scale, the surface-to-volume ratio is so great that the reagents acted on the experiment decrease. In combination with software, the analysis on these chips lower sample consumption, reduce cost, save experimental time, and increase data precision. The practical applications of lab-on-a-chip developed include, for example, biosensors for clinical detections, the control and optimal systems of chromatographic separations [18, 19], DNA analyzers based on capillary electrophoresis, portable equipment for "point-of-care" monitoring to remote healthcare of patients [4], and so on.

So far, capillary electrophoresis (CE) and capillary electrochromatography (CEC) are used mostly in the present approaches of separation in microfluidic chips. In order to offer a different method and to increase the efficiency and fasten the entire process during the separation on biological molecules, the usage of oscillating electroosmotic flow is proposed to enhance mass transport of solute and separation between different species. As a result, this research is aimed at investigating theoretically the physics and phenomena of mass transfer and separation of species by pulsatile electroosmotic flow. The effects on the mass transfer and separation of species due to various conditions will be studied systematically. The results will be helpful for the design of biochips. Also, the research is significant and has challenges theoretically.

1-3 Background and Literature Review

Although researches about the mass transport and separation of species enhanced by oscillating electroosmotic flows cannot be found so far, a number of discussions and applications about electroosmotic flows and pressure- or wall-driven oscillating flows to improve the mass transfer and separate species have been published in the past five decades. We then describe briefly the background and applications of these two fields.

Electroosmotic Flow

Researches of EOF in the early days focused mostly on the basic phenomenon of flow in a simple geometric channel, e.g., a straight cylindrical tube or two parallel plates. Recently, the further effects of inertia forces, pressure forces, and non-uniform zeta potential, accompanied with heat transfer, are considered. And the geometries of pipes are more complicated, for example, T-shape, U-shape, and so on. Unsteady EOF was also the points in recent researches.

Pressure-driven fully developed flows and heat transfer under electrokinetic effects in microchannels were discussed in 1997 and 1998. Mala et al. analyzed them in microchannels of two parallel plates theoretically and experimentally [20, 21] and Yang et al. in rectangular microchannels [22]. They researched streaming currents and streaming potentials caused by the interaction of EDL and the flow and then an inverse conduction current was induced. Later R-J Yang et al. investigated electroosmotic flows from entry region to fully developed region in microchannels of two parallel plates and 90^{o} bend [23, 24] in 2001. It was found that the entrance length of EOF was long than the one in the flow driven by pressure. And the thickness of EDL in the entry region was thinner than that in the fully developed region. On the other hand, in a research by Santiago, the effects of finite inertial and pressure forces in electroosmotic flows in two-dimensional microchannels was focused on in 2001 [25]. The flow was driven by pressure in addition to an impulsively started electrical field. In this research, the flow was divided into two regions: one was an inner region dominated by viscous and electrostatic forces and the other was an outer region dominated by inertial and pressure forces.

Effects of surface heterogeneity are also important phenomena in electroosmotic flows. They are used to enhance the efficiency of mixing. Stroock et al. presented EOF with patterned surface charges in rectangular microchannels in 2000 [26]. The directions of variation of the patterned surfaced charge were two: along the direction perpendicular to the electrical field and the one parallel to it. When the variation was parallel to the electrical field, a recirculating cellular flow was generated. Their results

demonstrated EOF would be induced by the surface patterned with charges. Ren, Escobedo and Li analyzed EOF in heterogeneous cylindrical microchannels [27] and developed a mixing process with one solution displacing another solution [28]. Further they used the circulation discussed by Stroock et al. to enhance the mixing of species in a T-shaped micromixer [29]. EOF with random zeta potential in a cylindrical capillary tube was studied by Gleeson [30]. The random zeta potential caused a plug flow of the mean velocity in the axial direction, like the results found by Stroock et al.

The electroosmotic flows mentioned above mostly are in steady state. However the unsteady EOF is more general in applications. Söderman and Jönsson investigated velocity profiles in different geometries with both temporal and spatial resolution in 1996 [31]. The electric field is applied as a step-function. González el at. discussed EOF induced by non-uniform AC electric fields in electrolytes on microelectrodes [32, 33]. The non-uniform field was generated by the electrodes interacting with the suspending fluid. Butta et al. solved the analytical solution of time periodic EOF in a two-dimensional straight channel [34]. Their results were compared to Stokes' second problem and found that they are much similar except near the wall. Erickson and Li. developed the steady time periodic velocity profile of EOF based on a Green's function formulation in a rectangular microchannel [35]. The oscillating laminar electrokinetic flow in infinitely extended circular microchannels was published by Bhattacharyya, Masliyah, and Yang [36]. A periodically external electrical field was applied to drive the flow. And the solution can be applied in EOF or in streaming potentials.

Dispersion and Pressure- or Wall-Driven Oscillating Flows

A pressure- or wall-driven oscillating flow in a channel can enhance the mass transport of species filled in the channel. The mechanism to improve the transport is similar to dispersion. We then discuss dispersion first.

Dispersion of soluble matter in solvent flowing slowly through a tube was first described in laminar and turbulent flows by Taylor in 1953 [11, 12] and by Aris in 1955 [14]. The famous phenomenon was called Taylor dispersion. He discussed the unclear descriptions in Griffiths' paper and supposed that a soluble substance spread out under the combination of molecular diffusion and the variation of velocity over the cross-section. A coefficient governing the dispersion, which was similar to a diffusion coefficient, was then derived. He then derived the condition under which dispersion of a solute in a stream of solvent can be used to measure molecular diffusion in 1954 [13]. Recently, an exact closed-form solution about dispersion of solute in laminar flow through a circular tube was solved by Mansour [37].

On the other hand, dispersion in EOF has been discussed in the last twenty years. Martin et al. and McEldoon et al. investigated axial dispersion capillary liquid chromatography with electroosmotic flow [38, 39]. In the paper by Griffiths and Nilson, the dispersion of a neutral passive solute in EOF was considered. The first-order concentration distribution and coefficient of axial dispersion were determined [40]. They also analyzed EOF and late-time solute transport for large zeta potentials analytically and numerically [41].

When dispersion is studied, we then consider the effects of oscillation on flows. Harris and Goren focused on axial diffusion in a cylinder with pressure-driven pulsed flow in 1967 [42]. The increase in the ratio of mass transfer in the system to that due to pure molecular diffusion was discussed in this paper theoretically and experimentally. Rice and Eagleton developed the mass transfer by laminar flow oscillations in 1970 [43]. The flow was driven by pressure in addition to an oscillating wall and then the two velocity distributions were solved in a complex way respectively. The total velocity profile was superposed 180° out of phase from the previous two profiles. Later the longitudinal dispersion of passive contaminant in pressure-driven oscillatory flows in tubes was reported by Chatwin [44]. Diffusion in oscillatory pipe flow was also studied by Watson in different cross-section tubes [45]. A research presented by Hydon and Pedley applied these well-developed theory on the motion of gas transport in the airway of the lung [46].

Separation

Oscillating flows are further applied to separate species. Kurzweg and Jaeger et al. published a series of researches about diffusional separation of gases or liquids by sinusoidal oscillations [47~52]. They defined a "tuned condition" under which the maximum mass transfer of gases occurred. And oscillations and a counter flow were combined to enhance the separation. In one of their researches, the theory of dispersion with oscillating flow was applied to analyze a rapid removal of contaminants from groundwater. A device called Enhanced Mass Pump (EMP) was used to improve the effectiveness.

In recent years, Thomas and Narayanan investigated the physics of oscillatory flow and its effect on the mass transfer and separation of species [53]. The time-averaged mass flow rate and the mass transfer ratio of faster diffusing species to slower one were derived. In the procedure of separation, the total mass transport of each species may be the same at some frequencies. These frequencies were called crossover frequencies. Difference between the enhanced mass transfer in boundary and pressure driven oscillatory flow was compared by Thomas and Narayanan in 2001[54].

1-4 Physical Models

Introduction of Our System [54]

Image a microscale capillary tube connecting a reservoir at each end. One of the reservoirs, say the one on the right, is considered to hold the pure fluid called the carrier while the other on the left holds a mixture of the carrier fluid with a dilute amount of a passive and neutral species as show in Fig. 1.1-2. A periodic electric field is applied along the axis. Suppose that the fluid in the tube oscillates with no net flow from one reservoir to the other. When the electroosmotic flow, provided that the frequency is not large, starts to work, a nearly inverse parabolic flow profile slowly oscillates back and forth in the tube with the fastest moving region at the boundary and the slowest region in the center. As shown in Fig. 1.1-3, in the first half of a cycle, the inverse parabolic flow profile produced in the tube causes radial concentration gradients. The dilute species then diffuse from the wall of the tube to the center, i.e., from the faster region to the slower one. The species thus moves from the mixture part to the pure fluid. In the second half of a cycle, the flow profile is reversed and radial concentration gradients in the pure fluid form. The species which have diffused in the first half cycle now is drawn back a little and diffuses from the center to the boundary. In the first half of the next cycle, the species in the faster region of the pure fluid is then convected down the tube and diffuses radially toward the center again. The species thus proceeds to move in this zigzag fashion down the tube and gives a higher transport of it than by pure molecular diffusion.

So far we can find that the mechanism of radial diffusion and axial convection is similar with the one in Taylor dispersion.

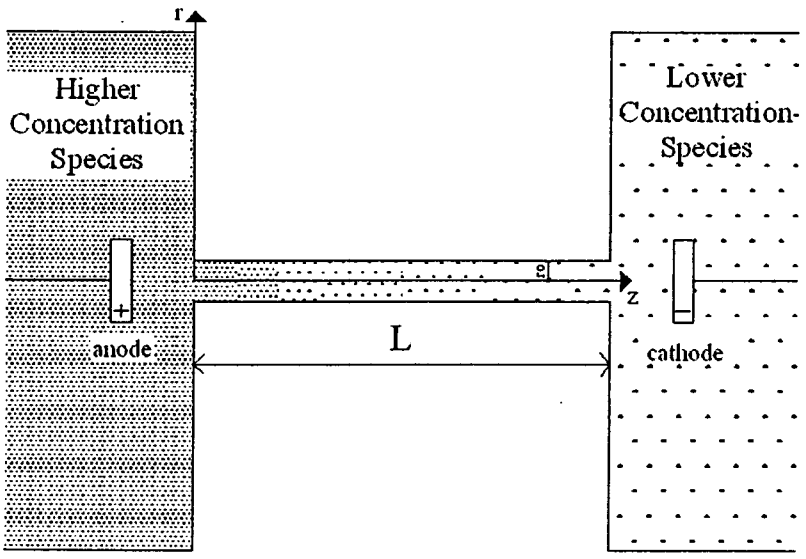

Fig. 1.1-2 Schema of our system

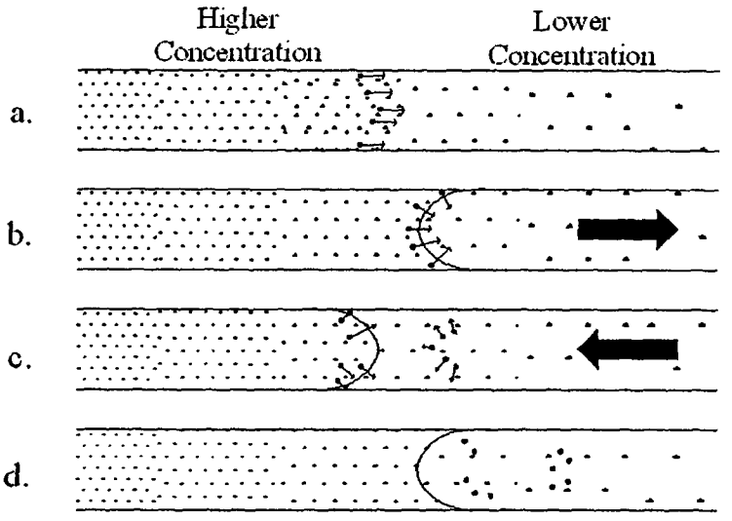

Fig. 1.1-3 Dispersion mechanism for a dilute species in electroosmosis flow

Now if another passive and dilute species were added to the mixture reservoir, the two species will transport in the same way but have different transferring time. Then the time constants of the system become very important due to the different diffusivity of the species, the frequency of oscillation, and the kinetic viscosity of the fluid. At different frequencies, the transfer of the faster diffusing species may be higher, lower, or the same as the slower one. We thus expect that at appropriate time constants we can use the system to separate the two species.

We will start to analyze the detail of the system in Chap. 2 and Chap. 3 including the physical model and mathematical analysis.

CHAPTER 2

ASSUMPTIONS AND FORMULATION

2-1 Assumptions

We have discussed the mechanism of our system in Sec. 1-1. Here our physical and mathematical model is constructed under some necessary assumptions which match the physical meanings

First of all, let us consider a symmetric capillary tube of radius r_0 with charged surface forming an EDL. The length of the tube is much longer compared to the radius, i.e., $L >> r_0$. And the capillary tube is filled with a dilute binary symmetric electrolyte solution with univalent charges. The coordinate system employed are shown in Fig. 1.1-3.

The following assumptions are made to simplify the mathematical manipulation and analysis.

Temperature field

The temperature around the tube is assumed uniform over the entire system.

No heat transfer and heat sources/sinks exist in the capillary tube.

Electric field

Assume a periodic electric field with frequency, ω, be applied along the capillary tube, i.e., along the z-direction. Here the frequency is not large and the electric field varies with time only, i.e., it is a spatially uniform, time-dependent electric field. [36]

And, the electrical potential across the EDL φ is assumed not affected by the periodic variation of the external electric field [34]. By further assuming the charged surface is homogeneous, and the zeta potential (see Appendix A) is uniform along the axial direction, i.e., the electrical potential resulted from the EDL is independent of z. Further the EDL around the capillary tube is not too thick to interact at the center of the tube, i.e., $r_0 > \lambda_D$ in which λ_D is the Debye length. Consider the EDL is thin.

The gravity is neglected, so the body force is resulted from electric field only.

Megnetic field, H

No magnetic field is applied and the characteristic time constant τ_s of the system

is much larger than the characteristic time constant τ_{em} for the electromagnetic wave propagation. Consequently, any magnetic field induced by the variation of the electric field is negligibly small. [36]

Flow field

An incompressible, Newtonian fluid with constant transport properties, e.g., constant viscosity, diffusivity, permittivity, etc., is considered. The flow is fully developed so the concentration of the electrolyte solution is in thermodynamic equilibrium. And the associated Reynolds number is small and then we neglect the inertia term in the Navier-Stokes' equation. Under the periodic assumption, there is no net flow across the capillary tube in order to compare meaningfully with the pure diffusion.

Concentration Field

No homogeneous chemical reaction in the bulk of the solution. Species in reservoirs are well-mixed. The time-averaged concentrations at inlet and outlet are constant and then the concentration difference is constant.

Initially, the flow is stationary. And the EDL is formed at a thermodynamic equilibrium state near the boundaries. Therefore the whole electrical potential ζ is only resulted from the EDL and then the ionic concentration is in Boltzmann distribution. [23]

Under there assumptions, we start to develop the governing equations.

2-2 Flow-Charts

In our model, we confront equations governing three fields: the electrical field, the velocity filed, and the concentration field of neutral species. Under the assumptions described in Sec. 2-1, the three governing equations are decoupled and can be solved analytically.

A series of flow charts are included in the following to illustrate the inter-relationship and sequence of solving these equations*.

* The details of deriving these equations inside the blocks are shown in Appendix B.

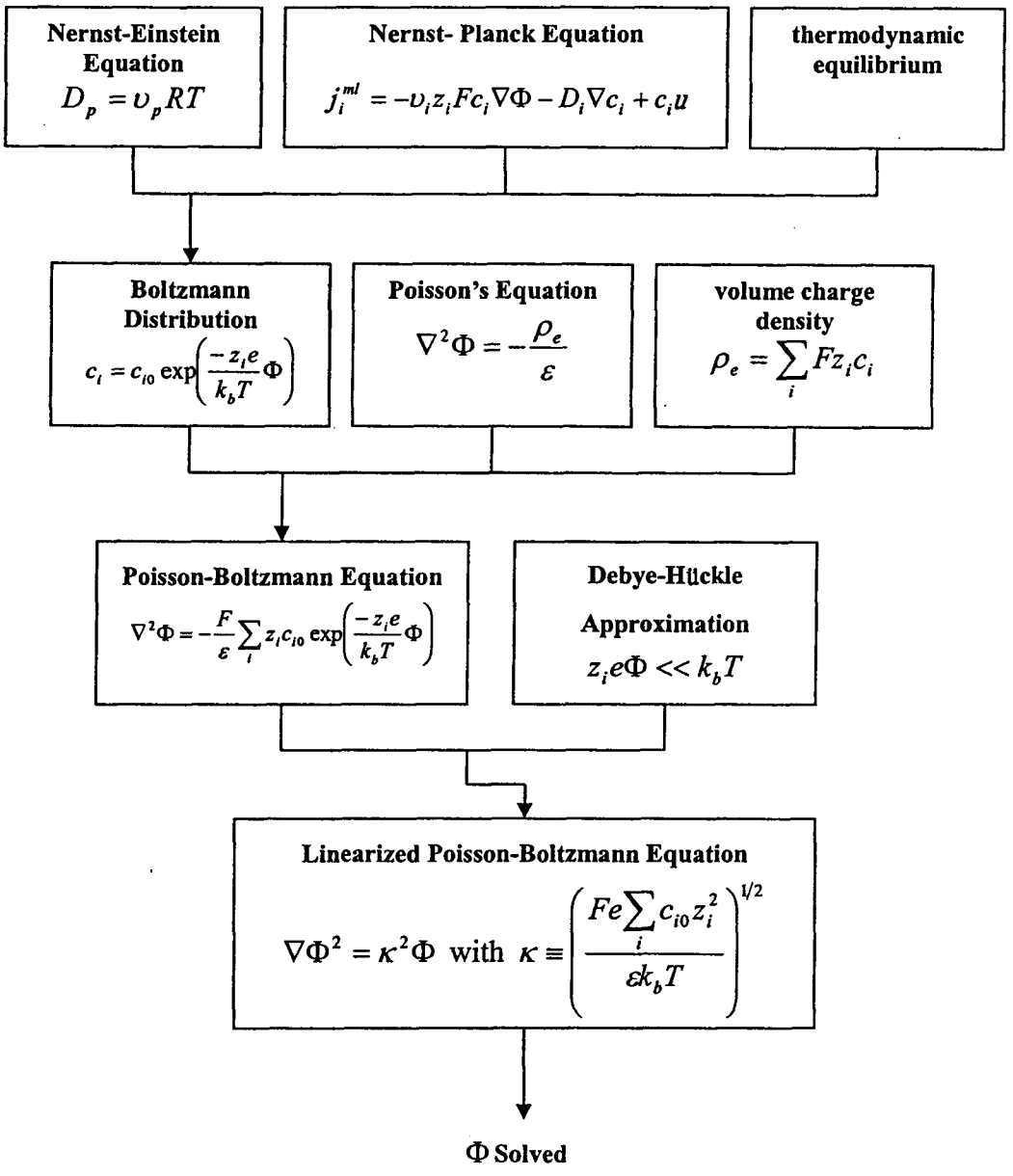

Fig. 2.2-1 The flow chart for solving the electrical field

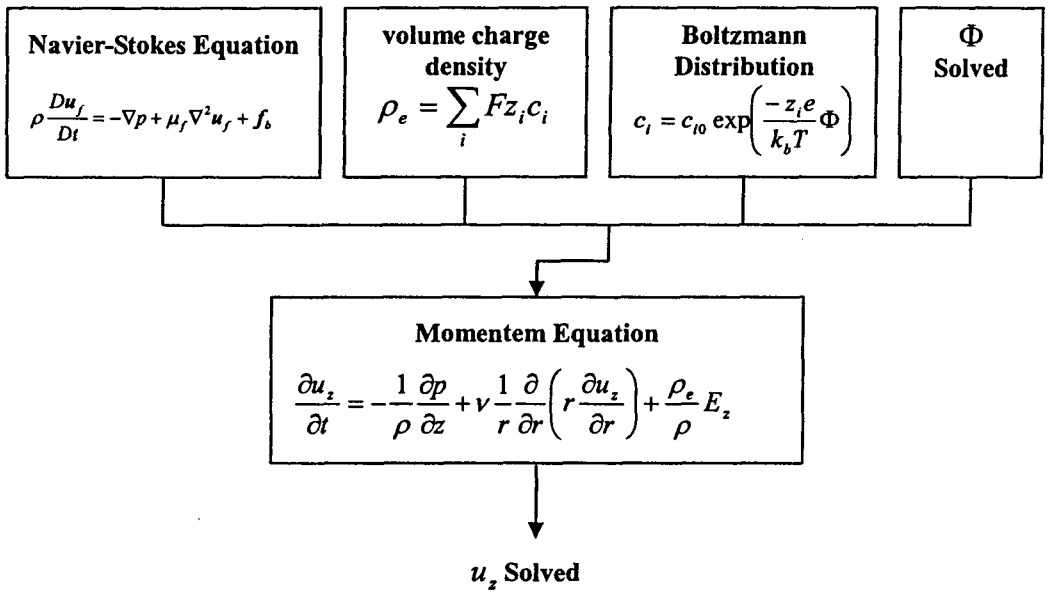

Fig. 2.2-2 The flow chart for solving the velocity field

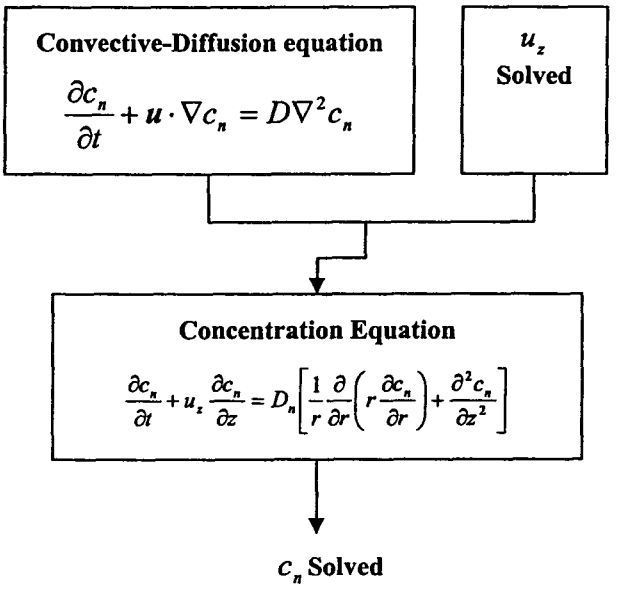

Fig. 2.2-3 The flow chart for solving the concentration field

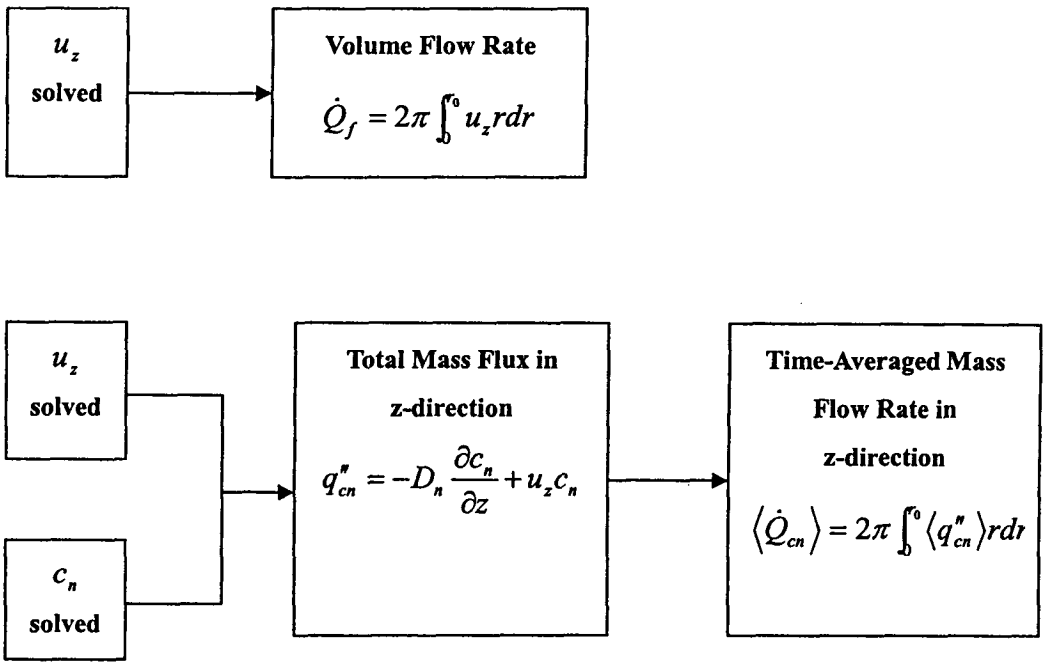

Fig. 2.2-4 The flow chart for solving the volume flow rate and mass flow rate

The meanings of the notations are listed below.

c_{i0} : concentration of species i in the bulk flow, molar / meter^3 (mol/m^3)

c_i : concentration of species i, molar / meter^3 (mol/m^3)

c_n : concentration of a neutral species n, molar / meter^3 (mol/m^3)

D_i : diffusivity or diffusion coefficient of species i, meter^2 / sec (m^2/s)

D_n : diffusivity or diffusion coefficient of species n, meter^2 / sec (m^2/s)

E_z : electric field intensity in z-direction, volt / meter (V/m)

f_b : body force, Newton / meter^3 (N/m^3)

j_i^{ml} : molar flux of species i, molar / meter^2 · sec $(mol/m^2 s)$

p : pressure, Pascal (Pa)

$\dot{Q}_{cn}$: mass flow rate of species n, mole / sec (mol/s)

$\dot{Q}_f$: volume flow rate of species n, mole / sec (mol/s)

q''_{cn} : mass flux of species n, mole / meter^{2}sec $(mol/m^2 s)$

r : the direction where the electrical potential varies, meter (m)

T : absolute temperature, Kelvin (K)

t : time, sec (s)

$\boldsymbol{u}$: mass average velocity, fluid velocity, meter/ sec (m/s)

u_z : fluid velocity in the flow direction z, meter / sec (m/s)

z : direction of axis in cylindrical coordinate, direction of flow, meter (m)

z_i : charge number of species i, dimensionless

Φ : total electric potential, volt (V)

ε : permittivity, absolute permittivity, farad / meter (F/m)

κ : Debye-Hückle parameter, 1 / meter $(1/m)$

μ_f : dynamic viscosity of fluid, Pascal • sec $(Pa \cdot s)$

ν : kinematic viscosity of solution, meter^2 / sec (m^2/s)

ρ_e : volume charge density, coulomb / meter^3 $\left(C/m^3\right)$

ρ : mass density of fluid, $\left(kg/m^3\right)$

υ_i : mobility of the particle i in solution, molar · meter^2 / joule · sec $\left(mol \cdot m^2/J \cdot s\right)$

Constant

e : elementary charge $=1.602\times10^{-19}$, coulomb (C)

F : Faraday's constant =96,487, coulomb / molar (C/mol)

k_b : Boltzmann constant $=1.381\times10^{-23}$, joule / Kelvin (J/K)

R : universal gas constant =8.3143, joule / molar · temperature $(J/mol \cdot K)$

After realizing the relationship of the whole equations, the governing equations applied in our model are then derived in Secs. 2-3 ~2-6.

2-3 The Electric Field

Based on the flow chart, we know the governing equation of the electric field is the linearized Poisson-Boltzmann equation. (See Appendix B)

$$\nabla\Phi^2 = \kappa^2\Phi \text{ with } \kappa \equiv \left(\frac{Fe\sum_i c_{i0} z_i^2}{\varepsilon k_b T} \right)^{1/2} \tag{B.6-3}$$

Under the assumption of a binary symmetric electrolyte solution filled in the capillary tube, i.e., $z_+ = -z_- \equiv z_b$ and $c_{+0} = c_{-0} = c_b$, the Debye-Hückle parameter becomes

$$\kappa = \left(\frac{2Fec_b z_b^2}{\varepsilon k_b T} \right)^{1/2} \tag{2.3-1}$$

where z_+ and z_- are charge numbers of positive and negative ions, and c_{+0} and c_{-0} are concentration of positive and negative ions in the bulk flow in binary symmetric solution respectively.

The total electrical potential now includes two sources: one is from DEL, the other from the applied electrical field.
Let the applied periodic electric field be:

$$\boldsymbol{E}_{ext}(t) = E_z(t)\boldsymbol{e}_k = E_{zA}\cos(\omega t)\boldsymbol{e}_k \tag{2.3-2}$$

Because of electrostatics, the external electrical field can be expressed by an electrical potential ϕ.

$$\boldsymbol{E}_{ext} = -\nabla\phi = -\left(\frac{\partial\phi}{\partial r}\boldsymbol{e}_r + \frac{\partial\phi}{\partial z}\boldsymbol{e}_k \right) \tag{2.3-3}$$

But $\boldsymbol{E}_{ext}$ only has the axial component, the $\frac{\partial\phi}{\partial r}$ term must be zero. Then

$$\frac{d\phi}{dz} = E_z \quad \Rightarrow \quad \phi(z,t) = zE_z(t) + const \tag{2.3-4}$$

So the electrical potential Φ at location (r,z) at a given time t is the superposition from the EDL and the external field.

$$\Phi(r,z,t) = \varphi(r) + \phi(z,t) = \varphi + (\phi_{z0} - zE_z) \tag{2.3-5}$$

where φ is the electric potential resulted from EDL, and ϕ_{zo} is the electrical potential at $z = 0$

Substitution of Eq. (2.3-5) into (B.2-3) leads to the equation below.

$$\frac{1}{r}\frac{d}{dr}\left(r\frac{d\varphi}{dr}\right)=\kappa^2\varphi \tag{2.3-6}$$

The boundary conditions of the linearized equation corresponding our model are:

$$\varphi(r_0)=\varphi_s \tag{2.3-7}$$

$$\varphi(0)=\varphi_0 \text{ : finite} \tag{2.3-8}$$

Equations (2.3-6), (2.3-7), and (2.3-8) are thus the simplified ones we solve practically in our model.

2-4 The Velocity Field

Based on the flow chart in Sec. 2-2 also, the momentum equation we need is derived from the Navier-Stokes' equation, volume charge density, Boltzmann distribution, and the total electrical potential solved. Now we do the procedure.

Because of incompressible flow and constant properties, the modified Navier-Stokes equation is:

$$\rho\frac{D\boldsymbol{u}}{Dt}=-\nabla p+\mu_f\nabla^2\boldsymbol{u}+\boldsymbol{f}_b \tag{2.4-1}$$

The meanings of these notations have been mentioned previously.

In our model, the body force is resulted from the electrical field only. And the electrical force in the flow field is Lorentz force. [7]:

$$\boldsymbol{f}_{bE}=\rho_e\boldsymbol{E}_{ext}=-\rho_e\nabla\Phi=-\rho_e\nabla(\varphi+\phi) \tag{2.4-2}$$

Here the total electrical potential is the one appeared in Sec. ().

Further because the flow is fully-developed, the radial velocity vanishs and the inertial term disappears for small Reynold's number.

Equation (2.4-1) in z-direction then becomes:

$$\frac{\partial u_z(r,t)}{\partial t}=-\frac{1}{\rho}\frac{\partial p}{\partial z}+\nu\frac{1}{r}\frac{\partial}{\partial r}\left(r\frac{\partial u_z}{\partial r}\right)+\frac{\rho_e}{\rho}\left(E_z-\frac{\partial\varphi}{\partial z}\right)=-\frac{1}{\rho}\frac{\partial p}{\partial z}+\nu\frac{1}{r}\frac{\partial}{\partial r}\left(r\frac{\partial u_z}{\partial r}\right)+\frac{\rho_e}{\rho}E_z \tag{2.4-3}$$

The boundary conditions are:

$$\text{no-slip}: u_z\big|_{r=r_0}=0 \tag{2.4-4}$$

$$\left.\frac{\partial u_z}{\partial r}\right|_{r=0} = 0 \tag{2.4-5}$$

Equations (2.4-3), (2.4-4), and (2.4-5) are then the ones we solved practically.

2-5 The Concentration Field of a Neutral Species

Again based on Sec. 2-2, the concentration equation we need is derived from the convective-diffusion equation in addition to the flow velocity solved.

The convective-diffusion equation of a neutral species is:

$$\frac{\partial c_n}{\partial t} + \boldsymbol{u}\cdot\nabla c_n = D_n \nabla^2 c_n \tag{2.5-1}$$

where c_n is concentration of a neutral species n and D_n is diffusion coefficient of the species with no chemical reaction.

Because of $u_r = 0$ in the fully developed flow, Eq. (2.5-1) becomes:

$$\frac{\partial c_n(r,z,t)}{\partial t} + u_z(r,t)\frac{\partial c_n}{\partial z} = D_n\left[\frac{1}{r}\frac{\partial}{\partial r}\left(r\frac{\partial c_n}{\partial r}\right) + \frac{\partial^2 c_n}{\partial z^2}\right] \tag{2.5-2}$$

The corresponding boundary conditions are:

$$\text{no penetration}: \left.\frac{\partial c_n}{\partial r}\right|_{r=r_0} = 0 \tag{2.5-3}$$

$$c_n|_{r=0} : \text{finite} \tag{2.5-4}$$

We also must specify the conditions at the "ends" of the tube. Know that the length of the tube is L with $L >> r_0$. We then take:

$$\begin{aligned} \langle c_n \rangle &= c_{n,in} \quad \text{at } z = 0 \\ \langle c_n \rangle &= c_{n,out} \quad \text{at } z = L \end{aligned} \tag{2.5-5}$$

Here the variable with brackets denotes its time averaged value.

Equations (2.5-2), (2.5-3), (2.5-4), and (2.5-5) are the ones we solved.

2-6 Volume Flow Rate and Mass Flow Rate

Volume Flow Rate

It is easy to solve the volume flow rate along the axial direction when we have the velocity of flow.

$$\dot{Q}_f = 2\pi \int_0^{r_0} u_z r dr \tag{2.6-1}$$

Because there is no net flow across the capillary tube, taking the time average, we have:

$$\langle \dot{Q}_f \rangle = 0 \tag{2.6-2}$$

Mass Flow Rate

Before we derive the equation of mass flow rate along the axial direction, the axial mass flux should be known first as shown in the flow chart.

The instantaneous axial mass flux of the concentration filed is contributed form diffusion of the species and convection by the flow field. [53, 54]

$$q''_{cn} = -D_n \frac{\partial c_n}{\partial z} + u_z c_n \tag{2.6-3}$$

However we are out of interest in the instantaneous values but the time averaged values.

Than taking the time average, we have

$$\langle q''_{cn}(r,z,t) \rangle = -D_n \frac{\partial \langle c_n(r,z,t) \rangle}{\partial z} + \langle u_z(r,t) c_n \rangle \tag{2.6-4}$$

Therefore the total rate of mass transfer is found by integrating the mass flux:

$$\dot{Q}_{cn} = 2\pi \int_0^{r_0} q''_{cn} r dr \tag{2.6-5}$$

Also taking the time average:

$$\langle \dot{Q}_{cn}(z,t) \rangle = 2\pi \int_0^{r_0} \langle q''_{cn}(r,z,t) \rangle r dr \tag{2.6-6}$$

Equation (2.6-6) is than the object of our paper.

CHAPTER 3

DIMENSIONAL ANALYSIS

AND ANALYTICAL SOLUTIONS

3-1 Nondimensionalization

3-1.1 Governing Equations and Boundary Conditions

All the governing equations and boundary conditions of this model has been derived in Chap. 2.

$$\begin{cases} \dfrac{1}{r}\dfrac{d}{dr}\left(r\dfrac{d\varphi}{dr}\right)=\kappa^2\varphi \\ \varphi(r_0)=\varphi_s \text{ and } \varphi(0)=\varphi_0 \text{ : finite} \end{cases} \qquad \text{(2.3-6) ~ (2.3-8)}$$

$$\begin{cases} \dfrac{\partial u_z(r,t)}{\partial t}=-\dfrac{1}{\rho}\dfrac{\partial p}{\partial z}+\nu\dfrac{1}{r}\dfrac{\partial}{\partial r}\left(r\dfrac{\partial u_z}{\partial r}\right)+\dfrac{\rho_e}{\rho}E_z(t) \\ \text{no-slip}: u_z\big|_{r=r_0}=0 \text{ and } \left.\dfrac{\partial u_z}{\partial r}\right|_{r=0}=0 \end{cases} \qquad \text{(2.4-3) ~ (2.4-5)}$$

$$\begin{cases} \dfrac{\partial c_n}{\partial t}+u_z\dfrac{\partial c_n}{\partial z}=D_n\left[\dfrac{1}{r}\dfrac{\partial}{\partial r}\left(r\dfrac{\partial c_n}{\partial r}\right)+\dfrac{\partial^2 c_n}{\partial z^2}\right] \\ \text{no penetration}: \left.\dfrac{\partial c_n}{\partial r}\right|_{r=r_0}=0, \text{ and } c_n\big|_{r=0} \text{ : finite} \\ \langle c_n\rangle=c_{n,in} \text{ at } z=0 \\ \langle c_n\rangle=c_{n,out} \text{ at } z=L \end{cases} \qquad \text{(2.5-2) ~ (2.5-5)}$$

Now we do the dimensional analysis to simplify our calculation.

First define the dimensionless variables:

characteristic length of the system: $r_0 \Rightarrow R\equiv\dfrac{r}{r_0}, Z\equiv\dfrac{z}{r_0}$ (3.1-1)

Debye-Hückle parameter: $\kappa=\left(\dfrac{2Fc_bz_b^2e}{\varepsilon k_bT}\right)^{1/2} \Rightarrow K\equiv\kappa r_0$ (3.1-2)

characteristic electrical potential: $\tilde{\varphi} \equiv \frac{k_b T}{z_b e} \Rightarrow \Psi \equiv \frac{\varphi}{\tilde{\varphi}} = \frac{z_b e}{k_b T}\varphi$ (3.1-3)

characteristic electrical field: $\tilde{E}_z \equiv \frac{k_b T}{z_b e r_0} \Rightarrow \mathbb{E}_z \equiv \frac{E_z}{\tilde{E}_z} = \frac{z_b e r_0}{k_b T} E_z$ (3.1-4)

characteristic concentration of species n: $c_{n,in}\text{-}c_{n,out} \Rightarrow C_n \equiv \frac{c_n}{c_{n,in}\text{-}c_{n,out}}$ (3.1-5)

characteristic velocity: $\tilde{u}_z \Rightarrow U_z \equiv \frac{u_z}{\tilde{u}_z}$ (3.1-6)

characteristic pressure: $\tilde{p} \Rightarrow P \equiv \frac{p}{\tilde{p}}$ (3.1-7)

characteristic time: $\tilde{t} \Rightarrow \tau \equiv \frac{t}{\tilde{t}}$ (3.1-8)

characteristic current density: $\tilde{\rho}_e \Rightarrow \varrho_e \equiv \frac{\rho_e}{\tilde{\rho}_e}$ (3.1-9)

characteristic volume flow rate: $\tilde{\dot{Q}}_f \Rightarrow \dot{\mathbb{Q}}_f \equiv \frac{\dot{Q}_f}{\tilde{\dot{Q}}_f}$ (3.1-10)

characteristic mass flux of species n: $\tilde{q}''_{cn} \Rightarrow Q''_{cn} \equiv \frac{q''_{cn}}{\tilde{q}''_{cn}}$ (3.1-11)

characteristic mass flow rate of species n: $\tilde{\dot{Q}}_{cn} \Rightarrow \dot{\mathbb{Q}}_{cn} \equiv \frac{\dot{Q}_{cn}}{\tilde{\dot{Q}}_{cn}}$ (3.1-12)

Here R is the direction of radius in dimensionless cylindrical coordinate, Z is the direction of axis in dimensionless cylindrical coordinate, and $c_{n,in} - c_{n,out}$ is the difference of concentration between the inlet and outlet of the tube. K means the ratio of the radius of the tube to Debye length. The larger K is, the thinner the diffuse layer is. $\Psi \equiv \frac{z_b e}{k_b T}\varphi$ means the ratio of the electrical force to the thermal force of the ions in EDL . At Small Ψ, we can use the Debye-Hückle approximation $\mathbb{E}_z = \frac{z_b e r_0}{k_b T} E_z$ means the electrical intensity compared to the one established by EDL.

Other variables, $\tilde{u}_z$, $\tilde{p}$, $\tilde{t}$, $\tilde{\rho}_e$, $\tilde{\dot{Q}}_f$, $\tilde{q}''_{cn}$, and $\tilde{\dot{Q}}_{cn}$, will be defined later when the dimensionless equations are presented.

Below we then derive the whole dimensionless equations by using these dimensionless variables.

Linearized Poisson-Boltzmann Equation

$$\frac{1}{(r_0R)}\frac{d}{d(r_0R)}\left((r_0R)\frac{d(\frac{k_bT}{z_be}\Psi)}{d(r_0R)}\right)=\kappa^2\frac{k_bT}{z_be}\Psi$$

$$\Rightarrow \frac{1}{R}\frac{d}{dR}\left(R\frac{d\Psi}{dR}\right)=(\kappa r_0)^2\Psi=K^2\Psi \tag{3.1-13}$$

BCs: $\Psi(1)=\Psi_s$ and $\Psi(0)$: finite (3.1-14)

where Ψ_0 is dimensionless electric potential from EDL in the bulk flow and Ψ_s is dimensionless electric potential on the wall of the capillary tube.

Momentum Equation

$$\frac{\partial(\tilde{u}_zU_z)}{\partial(\tilde{t}\,\tau)}=-\frac{1}{\rho}\frac{\partial(\tilde{p}P)}{\partial(r_0Z)}+\nu\frac{1}{(r_0R)}\frac{\partial}{\partial(r_0R)}\left((r_0R)\frac{\partial(\tilde{u}_zU_z)}{\partial(r_0R)}\right)+\frac{(\tilde{\rho}_e\varrho)}{\rho}(\frac{k_bT}{z_ber_0}\mathbb{E}_z)$$

$$\Rightarrow \frac{r_0^2}{\tilde{t}\,\nu}\frac{\partial U_z}{\partial\tau}=\frac{-\tilde{p}r_0}{\tilde{u}_z\mu_f}\frac{\partial P}{\partial Z}+\frac{1}{R}\frac{\partial}{\partial R}\left(R\frac{\partial U_z}{\partial R}\right)+\frac{\tilde{\rho}_ek_bTr_0}{\tilde{u}_z\mu_fz_be}\varrho_e\mathbb{E}_z$$

$$\because \frac{r_0^2}{\tilde{t}\,\nu},\frac{-\tilde{p}r_0}{\tilde{u}_z\mu_f},\frac{\tilde{\rho}_ek_bTr_0}{\tilde{u}_z\mu_fz_be}\text{ are dimensionless}$$

$$\Rightarrow \tilde{t}\equiv\frac{r_0^2}{\nu},\tilde{p}\equiv\frac{\tilde{u}_z\mu_f}{r_0},\tilde{\rho}_e\equiv\frac{\tilde{u}_zz_be\mu_f}{k_bTr_0} \tag{3.1-15}$$

On the other hand,

$$\rho_e=\frac{-2Fc_bz_b^2e}{k_bT}\varphi=\frac{-2Fc_bz_b^2e}{k_bT}\frac{k_bT\Psi}{z_be}=-2Fc_bz_b\Psi$$

$$\Rightarrow \varrho_e=\frac{\rho_e}{\tilde{\rho}_e}=\frac{k_bTr_0}{\tilde{u}_z\mu_fz_be}\rho_e=\frac{k_bTr_0}{\tilde{u}_z\mu_fz_be}(-2Fc_bz_b\Psi)=\frac{-2Fc_bk_bTr_0}{\tilde{u}_z\mu_fe}\Psi$$

$$\because \rho_e, \Psi \text{ are dimensionless} \Rightarrow \frac{-2Fc_b k_b T r_0}{\tilde{u}_z \mu_f e} \text{ is dimensionless}$$

$$\Rightarrow \tilde{u}_z \equiv \frac{2Fc_b k_b T r_0}{\mu_f e} \tag{3.1-16}$$

$$\therefore \rho_e = -\Psi$$

$$\therefore \frac{\partial U_z}{\partial \tau} = -\frac{\partial P}{\partial Z} + \frac{1}{R}\frac{\partial}{\partial R}\left(R\frac{\partial U_z}{\partial R}\right) - \Psi \mathbb{E}_z \tag{3.1-17}$$

$$\text{BCs: } U_z\big|_{R=1} = 0 \text{ and } \left.\frac{\partial U_z}{\partial R}\right|_{R=0} = 0 \tag{3.1-18}$$

Here $\tilde{t} \equiv \frac{r_0^2}{\nu}$, $\tilde{p} \equiv \frac{\tilde{u}_z \mu_f}{r_0}$, $\tilde{\rho}_e \equiv \frac{\tilde{u}_z z_b e \mu_f}{k_b T r_0}$, and $\tilde{u}_z \equiv \frac{2Fc_b k_b T r_0}{\mu_f e}$ are defined. $\tilde{t}$ means the characteristic diffusion time of fluid particles. $\tilde{u}_z$ means the velocity of fluid particles drawn by the ions which are driven by the thermal energy. $\tilde{p}$ means the pressure produced by these ions. $\tilde{\rho}_e = \frac{Fc_b}{e} z_b e$ means the total volume charge density in the bulk flow.

Further we define $\Omega \equiv \frac{\omega r_0^2}{\nu}$. This is the square of Womersley number which is the ratio of the characteristic diffusion time of fluid particles to the characteristic time of oscillation. A small Ω means that the transport by diffusion is slower than by convection driven from oscillation.

Concentration Equation

$$\frac{\partial((c_{n,in} - c_{n,out})C_n)}{\partial(r_0^2 \tau/\nu)} + (\tilde{u}_z U_z)\frac{\partial((c_{n,in} - c_{n,out})C_n)}{\partial(r_0 Z)}$$

$$= D_n\left[\frac{1}{(r_0 R)}\frac{\partial}{\partial(r_0 R)}\left((r_0 R)\frac{\partial((c_{n,in} - c_{n,out})C_n)}{\partial(r_0 R)}\right) + \frac{\partial^2((c_{n,in} - c_{n,out})C_n)}{\partial(r_0 R)^2}\right]$$

$$\Rightarrow \frac{\nu}{D_n}\frac{\partial C_n}{\partial \tau} + \frac{r_0 \tilde{u}_z}{D_n} U_z \frac{\partial C_n}{\partial Z} = \frac{1}{R}\frac{\partial}{\partial R}\left(R\frac{\partial C_n}{\partial R}\right) + \frac{\partial^2 C_n}{\partial Z^2}$$

$$\therefore S_c \frac{\partial C_n}{\partial \tau} + \tilde{P}_{eD} U_z \frac{\partial C_n}{\partial Z} = \frac{1}{R}\frac{\partial}{\partial R}\left(R\frac{\partial C_n}{\partial R}\right) + \frac{\partial^2 C_n}{\partial Z^2} \tag{3.1-19}$$

$$\text{BCs: } \left.\frac{\partial C_n}{\partial R}\right|_{R=1} = 0 \text{ and } C_n\big|_{R=0} : \text{finite} \tag{3.1-20}$$

$$\langle C_n \rangle = C_{n,in} \text{ at } Z = 0,\ \langle C_n \rangle = C_{n,out} \text{ at } Z = \frac{L}{r_0} \tag{3.1-21}$$

where S_c is Schmidt number and $\widetilde{P}_{eD} \equiv \frac{r_0 \widetilde{u}_z}{D_n}$ is Peclet number of diffusion. $C_{n,in}$ and $C_{n,out}$ are dimensionless concentrations of species *n* at the inlet and outlet of the capillary tube respectively.

So the dimensionless governing equations and boundary conditions are:

$$\begin{cases} \frac{1}{R}\frac{d}{dR}\left(R\frac{d\Psi(R)}{dR}\right) = (\kappa r_0)^2 \Psi = K^2 \Psi \\ \Psi(1) = \Psi_s, \Psi(0): \text{finite} \end{cases} \tag{3.1-13), (3.1-14}$$

$$\begin{cases} \frac{\partial U_z(R,\tau)}{\partial \tau} = -\frac{\partial P}{\partial Z} + \frac{1}{R}\frac{\partial}{\partial R}\left(R\frac{\partial U_z}{\partial R}\right) - \Psi \mathbb{E}_z \\ U_z(1,\tau) = 0, \frac{\partial U_z(0,\tau)}{\partial R} = 0 \end{cases} \tag{3.1-17), (3.1-18}$$

$$\begin{cases} S_c \frac{\partial C_n(R,Z,\tau)}{\partial \tau} + \widetilde{P}_{eD} U_z \frac{\partial C_n}{\partial Z} = \frac{1}{R}\frac{\partial}{\partial R}\left(R\frac{\partial C_n}{\partial R}\right) + \frac{\partial^2 C_n}{\partial Z^2} \\ \frac{\partial C_n(1,Z,\tau)}{\partial R} = 0,\ C_n(0,Z,\tau): \text{finite} \\ \langle C_n(R,0,\tau) \rangle = C_{n,in},\ \langle C_n(R, L/r_0, \tau) \rangle = C_{n,out} \end{cases} \tag{3.1-19) ~ (3.1-21}$$

3-1.2 Volume Flow Rate and Mass Flow Rate

Volume Flow Rate

$$\dot{Q}_f = 2\pi \int_0^{r_0} u_z r dr \Rightarrow \tilde{\dot{Q}}_f \dot{\mathbb{Q}}_f = 2\pi \int_0^1 (\tilde{u}_z U_z)(r_0 R) d(r_0 R) = 2\pi r_0^2 \tilde{u}_z \int_0^1 U_z R dR$$

$$\tilde{\dot{Q}}_f \equiv 2\pi r_0^2 \tilde{u}_z = \frac{4\pi F c_b k_b T r_0^3}{\mu e} \tag{3.1-23}$$

$$\therefore \ \dot{\mathbb{Q}}_f(\tau) = \int_0^1 U_z R dR \tag{3.1-23}$$

where $\tilde{\dot{Q}}_f$ means the reference volume flow rate.

Mass Flux

$$q''_{cn} = -D_n \frac{\partial c_n}{\partial z} + u_z c_n \Rightarrow Q''_{cn} \tilde{q}''_{cn} = -D_n \frac{\partial \left((c_{n,in} - c_{n,out}) C_n \right)}{\partial (r_0 Z)} + (\tilde{u}_z U_z)\left((c_{n,in} - c_{n,out}) C_n \right)$$

$$\tilde{q}''_{cn} \equiv \frac{D_n (c_{n,in} - c_{n,out})}{r_0} \tag{3-1.24}$$

$$\therefore \ Q''_{cn}(R, Z, \tau) = -\frac{\partial C_n}{\partial Z} + \frac{\tilde{u}_z r_0}{D_n}(U_z C_n) = -\frac{\partial C_n}{\partial Z} + \tilde{P}_{eD}(U_z C_n) \tag{3-1.25}$$

where $\tilde{q}''_{cn}$ means the mass flux by pure diffusion.

Then

$$\langle Q''_{cn}(R, Z, \tau) \rangle = \left\langle -\frac{\partial C_n}{\partial Z} + \tilde{P}_{eD}(U_z C_n) \right\rangle = -\frac{\partial \langle C_n \rangle}{\partial Z} + \tilde{P}_{eD} \langle U_z C_n \rangle \tag{3-1.26}$$

Mass Flow Rate

$$\dot{Q}_{cn} = 2\pi \int_0^{r_0} q''_{cn} r dr \Rightarrow \dot{\mathbb{Q}}_{cn} \tilde{\dot{Q}}_{cn} = 2\pi \int_0^1 (Q''_{cn} \tilde{q}''_{cn})(r_0 R) d(r_0 R)$$

$$\tilde{\dot{Q}}_{cn} \equiv 2\pi r_0^2 \tilde{q}''_{cn} = 2\pi r_0^2 \frac{D_n (c_{n,in} - c_{n,out})}{r_0} = 2\pi r_0 D_n (c_{n,in} - c_{n,out}) \tag{3-1.27}$$

$$\therefore \ \dot{\mathbb{Q}}_{cn}(Z, \tau) = \int_0^1 Q''_{cn} R dR \tag{3-1.28}$$

where $\tilde{\dot{Q}}_{cn}$ means the mass flow rate by pure diffusion.

Then

$$\langle \dot{\mathbb{Q}}_{cn}(Z, \tau) \rangle = \left\langle \int_0^1 Q''_{cn} R dR \right\rangle = \int_0^1 \langle Q''_{cn} \rangle R dR \tag{3-1.29}$$

Therefore Eqs. (3-1.23), (3-1.26), and (3-1.29) are the dimensionless equations we need. In the following sections, we will solve the exact solutions from these equations.

3-2 Some Definitions for Simplification

Before solving the governing equations actually, we define some notations which appear repeatedly in our calculating process. Using them in the analytical procedure, we can read the equations much clearly. (See Appendix C)

Coefficients

Here we use simple notations to represent the eiganvalues of the Bessel functions and some calculations of these eiganvalues.

$$\alpha_I \equiv \sqrt{i\Omega} \Rightarrow \overline{\alpha}_I \equiv \sqrt{-i\Omega} \tag{3.2-1}$$

$$\alpha_J \equiv \sqrt{-i\Omega} \Rightarrow \overline{\alpha}_J \equiv \sqrt{i\Omega} \tag{3.2-2}$$

$$\beta_I \equiv \sqrt{i\Omega S_c} \Rightarrow \overline{\beta}_I \equiv \sqrt{-i\Omega S_c} \tag{3.2-3}$$

$$\beta_J \equiv \sqrt{-i\Omega S_c} \Rightarrow \overline{\beta}_J \equiv \sqrt{i\Omega S_c} \tag{3.2-4}$$

$$cfa1(\Omega) \equiv \frac{1}{i\Omega} \tag{3.2-5}$$

$$cfa2(\Omega) \equiv \frac{1}{K^2 - i\Omega} \Rightarrow \overline{cfa2}(\Omega) \equiv \frac{1}{K^2 + i\Omega} \tag{3.2-6}$$

$$cfa3(\Omega, S_c) \equiv cfa1 - cfa5 = \frac{1}{i\Omega} - \frac{1}{i\Omega S_c} \tag{3.2-7}$$

$$cfa4(\Omega, S_c) \equiv cfa2 - cfa6 = \frac{1}{K^2 - i\Omega} - \frac{1}{K^2 - i\Omega S_c} \tag{3.2-8a}$$

$$\overline{cfa4}(\Omega, S_c) \equiv \overline{cfa2} - \overline{cfa6} = \frac{1}{K^2 + i\Omega} - \frac{1}{K^2 + i\Omega S_c} \tag{3.2-8b}$$

$$cfa5(\Omega, S_c) \equiv \frac{1}{i\Omega S_c} \tag{3.2-9}$$

$$cfa6(\Omega, S_c) \equiv \frac{1}{K^2 - i\Omega S_c} \Rightarrow \overline{cfa6}(\Omega, S_c) \equiv \frac{1}{K^2 + i\Omega S_c} \tag{3.2-10}$$

$$cfb1(\Omega) \equiv \frac{1}{K^2 - \overline{\alpha}_I^2} \text{ or } \equiv \frac{-1}{(iK)^2 - \overline{\alpha}_J^2} = \frac{1}{K^2 + i\Omega} \tag{3.2-11}$$

$$cfb2(\Omega,S_c)\equiv\frac{1}{K^2-\overline{\beta}_I^2}\ \text{or}\ \equiv\frac{-1}{(iK)^2-\overline{\beta}_J^2}=\frac{1}{K^2+i\Omega S_c} \tag{3.2-12}$$

$$cfb3(\Omega)\equiv\frac{1}{\alpha_I{}^2-K^2}\ \text{or}\ \equiv\frac{-1}{\alpha_J^2-(-iK)^2}=\frac{1}{i\Omega-K^2} \tag{3.2-13}$$

$$cfb4(\Omega)\equiv\frac{1}{\alpha_I{}^2-\overline{\alpha}_I^2}\ \text{or}\ \equiv\frac{-1}{\alpha_J^2-\overline{\alpha}_J^2}=\frac{1}{2i\Omega} \tag{3.2-14}$$

$$cfb5(\Omega,S_c)\equiv\frac{1}{\alpha_I{}^2-\overline{\beta}_I^2}\ \text{or}\ \equiv\frac{-1}{\alpha_J^2-\overline{\beta}_J^2}=\frac{1}{i\Omega(1+S_c)} \tag{3.2-15}$$

$$cfb6(\Omega,S_c)\equiv\frac{1}{\overline{\beta}_I^2}\ \text{or}\ \equiv\frac{-1}{\overline{\beta}_J^2} \tag{3.2-16}$$

$$\begin{aligned}cfb7(\Omega,S_c)&=-cfb2+cfb5-cfb3\\&=-\frac{1}{K^2+i\Omega S_c}+\frac{1}{i\Omega(1+S_c)}-\frac{-1}{K^2-i\Omega}\end{aligned} \tag{3.2-17}$$

$$\begin{aligned}cfb8(\Omega,S_c)&=cfb6+cfb5-cfb3\\&=-\frac{1}{i\Omega S_c}+\frac{1}{i\Omega(1+S_c)}-\frac{-1}{K^2-i\Omega}\end{aligned} \tag{3.2-18}$$

$$\begin{aligned}cfb9(\Omega,S_c)&=cfb6+cfb5-cfb4\\&=-\frac{1}{i\Omega S_c}+\frac{1}{i\Omega(1+S_c)}-\frac{1}{2i\Omega}\end{aligned} \tag{3.2-19}$$

$$\begin{aligned}cfb10(\Omega,S_c)&=-cfb2+cfb5+cfb1-cfb4\\&=-\frac{1}{K^2+i\Omega S_c}+\frac{1}{i\Omega(1+S_c)}+\frac{1}{K^2+i\Omega}-\frac{1}{2i\Omega}\end{aligned} \tag{3.2-20}$$

Some Bessel Functions

During the analytical procedure, some relations of Bessel functions appear repeatedly. We then use some simple notations to represent these relations in order to simplify the equations.

$$bf1(R)\equiv\frac{I_0(KR)}{I_0(K)}=\frac{J_0(iKR)}{J_0(iK)}\Rightarrow\overline{bf1}(R)\equiv\frac{I_0(KR)}{I_0(K)}=\frac{J_0(-iKR)}{J_0(-iK)} \tag{3.2-21}$$

$$bf2(R,\Omega)\equiv\frac{I_0(\alpha_I R)}{I_0(\alpha_I)}=\frac{J_0(\alpha_J R)}{J_0(\alpha_J)}\Rightarrow\overline{bf2}(R,\Omega)\equiv\frac{I_0(\overline{\alpha}_I R)}{I_0(\overline{\alpha}_I)}=\frac{J_0(\overline{\alpha}_J R)}{J_0(\overline{\alpha}_J)} \tag{3.2-22}$$

$$bf3(R,\Omega,S_c)\equiv\frac{I_0(\beta_I R)}{\beta_I I_1(\beta_I)}=\frac{-J_0(\beta_J R)}{\beta_J J_1(\beta_J)}\Rightarrow\overline{bf3}(R,\Omega,S_c)\equiv\frac{I_0(\overline{\beta}_I R)}{\overline{\beta}_I I_1(\overline{\beta}_I)}=\frac{-J_0(\overline{\beta}_J R)}{\overline{\beta}_J J_1(\overline{\beta}_J)} \tag{3.2-23}$$

$$bf4 \equiv \frac{KI_1(K)}{I_0(K)} = \frac{-(iK)J_1(iK)}{J_0(iK)} \Rightarrow \overline{bf4} \equiv \frac{KI_1(K)}{I_0(K)} = \frac{-(-iK)J_1(-iK)}{J_0(-iK)} \tag{3.2-24}$$

$$bf5 \equiv \frac{I_1(K)}{KI_0(K)} = \frac{J_1(iK)}{(iK)J_0(iK)} \Rightarrow \overline{bf5} \equiv \frac{I_1(K)}{KI_0(K)} = \frac{J_1(-iK)}{(-iK)J_0(-iK)} \tag{3.2-25}$$

$$bf6(\Omega) \equiv \frac{\alpha_I I_1(\alpha_I)}{I_0(\alpha_I)} = \frac{-\alpha_J J_1(\alpha_J)}{J_0(\alpha_J)} \Rightarrow \overline{bf6}(\Omega) \equiv \frac{\overline{\alpha}_I I_1(\overline{\alpha}_I)}{I_0(\overline{\alpha}_I)} = \frac{-\overline{\alpha}_J J_1(\overline{\alpha}_J)}{J_0(\overline{\alpha}_J)} \tag{3.2-26}$$

$$bf7(\Omega) \equiv \frac{I_1(\alpha_I)}{\alpha_I I_0(\alpha_I)} = \frac{J_1(\alpha_J)}{\alpha_J J_0(\alpha_J)} \Rightarrow \overline{bf7}(\Omega) \equiv \frac{I_1(\overline{\alpha}_I)}{\overline{\alpha}_I I_0(\overline{\alpha}_I)} = \frac{J_1(\overline{\alpha}_J)}{\overline{\alpha}_J J_0(\overline{\alpha}_J)} \tag{3.2-27}$$

$$bf8(\Omega, S_c) \equiv \frac{I_0(\beta_I)}{\beta_I I_1(\beta_I)} = \frac{-J_0(\beta_J)}{\beta_J J_1(\beta_J)} \Rightarrow \overline{bf8}(\Omega, S_c) \equiv \frac{I_0(\overline{\beta}_I)}{\overline{\beta}_I I_1(\overline{\beta}_I)} = \frac{-J_0(\overline{\beta}_J)}{\overline{\beta}_J J_1(\overline{\beta}_J)} \tag{3.2-28}$$

Some Integrals about Bessel Functions

We also encounter repeating integrals of Bessel functions. Again, we use simple notations to represent them. (See Appendix C)

$$ibf\_a1 = \int_0^1 (bf1) RdR = bf5 \tag{3.2-29}$$

$$ibf\_a2 = \int_0^1 (\overline{bf1}) RdR = \overline{bf5} \tag{3.2-30}$$

$$ibf\_a3(\Omega) = \int_0^1 (bf2) RdR = bf7 \tag{3.2-31}$$

$$ibf\_a4(\Omega) = \int_0^1 (\overline{bf2}) RdR = \overline{bf7} \tag{3.2-32}$$

$$ibf\_a5(\Omega, S_c) = \int_0^1 (\overline{bf3}) RdR = cfb6 \tag{3.2-33}$$

$$ibf\_b1 = \int_0^1 (bf1)(\overline{bf1}) RdR = \frac{1}{2}[1 - bf4bf5] \tag{3.2-34}$$

$$ibf\_b2(\Omega) = \int_0^1 (bf1)(\overline{bf2}) RdR = cfb1(bf4 - \overline{bf6}) \tag{3.2-25}$$

$$ibf\_b3(\Omega, S_c) = \int_0^1 (bf1)(\overline{bf3}) RdR = cfb2(bf4\overline{bf8} - 1) \tag{3.2-26}$$

$$ibf\_b4(\Omega) = \int_0^1 (bf2)(\overline{bf1}) RdR = cfb3(bf6 - \overline{bf4}) \tag{3.2-27}$$

$$ibf\_b5(\Omega) = \int_0^1 (bf2)(\overline{bf2}) RdR = cfb4(bf6 - \overline{bf6}) \tag{3.2-38}$$

$$ibf\_b6(\Omega, S_c) = \int_0^1 (bf2)(\overline{bf3}) RdR = cfb5(bf6\overline{bf8} - 1) \tag{3.2-39}$$

$$ibf\_c1 = \int_0^1 RdR = \frac{R^2}{2}\Big|_0^1 = \frac{1}{2} \tag{3.2-40}$$

Afetr these functions are defined, we can analyze the mathematical calculation more conveniently. These definitions are then used in later sections.

3-3 The Electrical Potential

We first solve the analytical solution of the electrical potential resulted from EDL.

$$\begin{cases} \frac{1}{R}\frac{d}{dR}\left(R\frac{d\Psi(R)}{dR}\right)-K^2\Psi=0 \\ \Psi(1)=\Psi_s,\Psi(0):\text{finite} \end{cases} \qquad (3.1\text{-}13),\ (3.1\text{-}14)$$

The equation has the form of Bessel's equation of order zero with the eigenvalue $\lambda_\Psi = -K^2 < 0$. So the solution is the modified Bessel function of zero order:

$$\Psi(R)=\Psi_A I_0(KR)+\Psi_B K_0(KR) \qquad (3.3\text{-}1)$$

where I_0 and K_0 are the first and second kind modified solutions of Bessel function of zero order respectively. Ψ_A and Ψ_B and integral constants.

Applying the boundary conditions:

$$\Psi(0)\text{is finite} \quad \therefore \Psi_B = 0 \quad \text{because } K_0|_{R=0} \text{ is infinite} \qquad (3.3\text{-}2)$$

$$\Psi(1)=\Psi_A I_0(KR)=\Psi_s \quad \therefore \Psi_A = \frac{\Psi_s}{I_0(K)} \qquad (3.3\text{-}3)$$

Therefore,

$$\Psi(R)=\Psi_s\frac{I_0(KR)}{I_0(K)}=\Psi_s\frac{J_0(iKR)}{J_0(iK)}=\Psi_s bf1 \qquad (3.3\text{-}4)$$

where J_0 the first kind solution of Bessel function of zero order.

3-4 The Velocity Profile

After knowing the distribution of the ionic electrical potential, the following quantity analyzed is the fluid velocity. The resulting expressions are similar with those obtained by Uchida [55].

The dimensionless governing equation and boundary conditions of the flow field are:

$$\begin{cases} \dfrac{\partial U_z(R,\tau)}{\partial \tau} = -\dfrac{\partial P}{\partial Z} + \dfrac{1}{R}\dfrac{\partial}{\partial R}\left(R\dfrac{\partial U_z}{\partial R}\right) - \Psi \mathbb{E}_z \\ U_z(1,\tau) = 0, \dfrac{\partial U_z(0,\tau)}{\partial R} = 0 \end{cases} \qquad (3.1\text{-}17),\ (3.1\text{-}18)$$

Complex variables are used to seek an analytical solution of the velocity profile [See Appendix C].

Define

$$\mathbb{E}_z(\tau,\Omega) \equiv \mathrm{Re}\left[E_z^*(\Omega)e^{i\Omega\tau}\right] \qquad (3.4\text{-}1)$$

$$-\frac{\partial P(Z,\tau,\Omega)}{\partial Z} \equiv \mathrm{Re}\left[P^*(Z,\Omega)e^{i\Omega\tau}\right] \qquad (3.4\text{-}2)$$

$$U_z(R,\tau,\Omega) \equiv \mathrm{Re}\left[U_z^*(R,\Omega)e^{i\Omega\tau}\right] \qquad (3.4\text{-}3)$$

where E_z^*, P^*, and U_z^* are all complex functions (See Appendix C).

Substitute above into the dimensionless momentum equation:

$$\begin{cases} (i\Omega)\left(U_z^* e^{i\Omega\tau}\right) = P^* e^{i\Omega\tau} + \dfrac{\partial^2 U_z^*}{\partial R^2} e^{i\Omega\tau} + \dfrac{1}{R}\dfrac{\partial U_z^*}{\partial R} e^{i\Omega\tau} - \Psi E_z^* e^{i\Omega\tau} \\ \Rightarrow \dfrac{\partial^2 U_z^*}{\partial R^2} + \dfrac{1}{R}\dfrac{\partial U_z^*}{\partial R} - i\Omega U_z^* = -P^* + \Psi E_z^* \\ U_z^*(1,\tau,\Omega) = 0, \dfrac{\partial U_z^*(0,\tau,\Omega)}{\partial R} = 0 \end{cases} \qquad (3.4\text{-}4)$$

It can be seen this is a non-homogeneous modified Bessel function of zero order with the eiganvalue $\alpha_I \equiv \sqrt{i\Omega}$ or $\alpha_J \equiv \sqrt{-i\Omega}$. Then the solution has the form:

$$U_z^* = U_A I_0\left(\sqrt{i\Omega}R\right) + U_B K_0\left(\sqrt{i\Omega}R\right) + U_{z,pt}^*$$

$$\text{or } = U_A J_0\left(\sqrt{-i\Omega}R\right) + U_B Y_0\left(\sqrt{-i\Omega}R\right) + U_{z,pt}^*$$

$$\Rightarrow \frac{\partial U_z^*}{\partial R} = U_A\left(\sqrt{i\Omega}\right) I_1\left(\sqrt{i\Omega}R\right) - U_B\left(\sqrt{i\Omega}\right) K_1\left(\sqrt{i\Omega}R\right) + \frac{\partial U_{z,pt}^*}{\partial R}$$

where U_A and U_B and integral constants.

We find the particular solution is

$$U^*_{z,pt} = \frac{P^*}{i\Omega} + \frac{\Psi E^*_z}{K^2 - i\Omega} \tag{3.4-5}$$

Check:

Substitute the particular solution into Eq.(3.4-4)

$$\begin{aligned}
&\frac{\partial^2 U^*_{z,pt}}{\partial R^2} + \frac{1}{R}\frac{\partial U^*_{z,pt}}{\partial R} - i\Omega U^*_{z,pt} \\
&= \frac{\partial^2\left(\frac{P^*}{i\Omega} + \frac{\Psi E^*_z}{K^2 - i\Omega}\right)}{\partial R^2} + \frac{1}{R}\frac{\partial\left(\frac{P^*}{i\Omega} + \frac{\Psi E^*_z}{K^2 - i\Omega}\right)}{\partial R} - i\Omega\left(\frac{P^*}{i\Omega} + \frac{\Psi E^*_z}{K^2 - i\Omega}\right) \\
&= \frac{E^*_z}{K^2 - i\Omega}\left(\frac{\partial^2\Psi}{\partial R^2} + \frac{1}{R}\frac{\partial\Psi}{\partial R}\right) - i\Omega\left(\frac{P^*}{i\Omega} + \frac{\Psi E^*_z}{K^2 - i\Omega}\right) \\
&= \frac{E^*_z}{K^2 - i\Omega}\left(K^2\Psi\right) - \left(P^* + \frac{i\Omega\Psi E^*_z}{K^2 - i\Omega}\right) \\
&= -P^* + \Psi E^*_z
\end{aligned} \tag{3.4-6}$$

Then

$$\begin{aligned}
&U^*_z = U_A I_0\left(\sqrt{i\Omega}R\right) + U_B K_0\left(\sqrt{i\Omega}R\right) + \left(\frac{P^*}{i\Omega} + \frac{\Psi E^*_z}{K^2 - i\Omega}\right) \\
&\Rightarrow \frac{\partial U^*_z}{\partial R} = U_A\left(\sqrt{i\Omega}\right) I_1\left(\sqrt{i\Omega}R\right) - U_B\left(\sqrt{i\Omega}\right) K_1\left(\sqrt{i\Omega}R\right) + \frac{E^*_z}{K^2 - i\Omega}\frac{\partial\Psi}{\partial R} \\
&\quad = U_A\left(\sqrt{i\Omega}\right) I_1\left(\sqrt{i\Omega}R\right) - U_B\left(\sqrt{i\Omega}\right) K_1\left(\sqrt{i\Omega}R\right) + \frac{E^*_z}{K^2 - i\Omega}\left(\Psi_s\frac{KI_1(KR)}{I_0(K)}\right)
\end{aligned}$$

Applying the boundary conditions:

1. $\left.\frac{\partial U^*_z}{\partial R}\right|_{R=0} = 0$: $U_B = 0$ because $K_1|_{R=0}$ is infinite and $I_1(0) = 0$. (3.4-7)

2. $U^*_z|_{R=1} = 0$:

$$\begin{aligned}
&U^*_z = U_A I_0\left(\sqrt{i\Omega}\right) + \left(\frac{P^*}{i\Omega} + \frac{\Psi_s E^*_z}{K^2 - i\Omega}\right) = U_A J_0\left(\sqrt{-i\Omega}\right) + \left(\frac{P^*}{i\Omega} + \frac{\Psi_s E^*_z}{K^2 - i\Omega}\right) = 0 \\
&\Rightarrow U_A = \frac{-1}{I_0\left(\sqrt{i\Omega}\right)}\left(\frac{P^*}{i\Omega} + \frac{\Psi_s E^*_z}{K^2 - i\Omega}\right) = \frac{-1}{J_0\left(\sqrt{-i\Omega}\right)}\left(\frac{P^*}{i\Omega} + \frac{\Psi_s E^*_z}{K^2 - i\Omega}\right)
\end{aligned} \tag{3.4-8}$$

Therefore

$$
\begin{aligned}
U_z^*(R,\Omega) &= -\left(\frac{P^*}{i\Omega}+\frac{\Psi_s E_z^*}{K^2-i\Omega}\right)\frac{I_0\left(\sqrt{i\Omega}R\right)}{I_0\left(\sqrt{i\Omega}\right)}+\left(\frac{P^*}{i\Omega}+\frac{\Psi E_z^*}{K^2-i\Omega}\right) \\
&= \frac{P^*}{i\Omega}\left(1-\frac{I_0\left(\sqrt{i\Omega}R\right)}{I_0\left(\sqrt{i\Omega}\right)}\right)+\frac{\Psi_s E_z^*}{K^2-i\Omega}\left(\frac{I_0(KR)}{I_0(K)}-\frac{I_0\left(\sqrt{i\Omega}R\right)}{I_0\left(\sqrt{i\Omega}\right)}\right) \\
&= \frac{P^*}{i\Omega}\left(1-\frac{I_0(\alpha_I R)}{I_0(\alpha_I)}\right)+\frac{\Psi_s E_z^*}{K^2-i\Omega}\left(\frac{I_0(KR)}{I_0(K)}-\frac{I_0(\alpha_I R)}{I_0(\alpha_I)}\right) \\
\text{or } &= \frac{P^*}{i\Omega}\left(1-\frac{J_0\left(\sqrt{-i\Omega}R\right)}{J_0\left(\sqrt{-i\Omega}\right)}\right)+\frac{\Psi_s E_z^*}{K^2-i\Omega}\left(\frac{J_0(iKR)}{J_0(iK)}-\frac{J_0\left(\sqrt{-i\Omega}R\right)}{J_0\left(\sqrt{-i\Omega}\right)}\right) \\
&= \frac{P^*}{i\Omega}\left(1-\frac{J_0(\alpha_J R)}{J_0(\alpha_J)}\right)+\frac{\Psi_s E_z^*}{K^2-i\Omega}\left(\frac{J_0(iKR)}{J_0(iK)}-\frac{J_0(\alpha_J R)}{J_0(\alpha_J)}\right) \\
&= \frac{P^*}{i\Omega}(1-bf2)+\frac{\Psi_s E_z^*}{K^2-i\Omega}(bf1-bf2)
\end{aligned}
\tag{3.4-9}
$$

Define $U_z^* \equiv U_{zP}^* P^* + U_{zE}^* E_z^*$

then

$$
\begin{aligned}
U_{zP}^*(R,\Omega) &= \frac{1}{i\Omega}\left(1-\frac{I_0\left(\sqrt{i\Omega}R\right)}{I_0\left(\sqrt{i\Omega}\right)}\right) \\
&= \frac{1}{i\Omega}\left(1-\frac{J_0\left(\sqrt{-i\Omega}R\right)}{J_0\left(\sqrt{-i\Omega}\right)}\right) \\
&= cfa1(1-bf2)
\end{aligned}
\tag{3.4-10}
$$

$$
\begin{aligned}
U_{zE}^*(R,\Omega) &= \frac{\Psi_s}{K^2-i\Omega}\left(\frac{I_0(KR)}{I_0(K)}-\frac{I_0\left(\sqrt{i\Omega}R\right)}{I_0\left(\sqrt{i\Omega}\right)}\right) \\
&= \frac{\Psi_s}{K^2-i\Omega}\left(\frac{J_0(iKR)}{J_0(iK)}-\frac{J_0\left(\sqrt{-i\Omega}R\right)}{J_0\left(\sqrt{-i\Omega}\right)}\right) \\
&= \Psi_s cfa2(bf1-bf2)
\end{aligned}
\tag{3.4-11}
$$

As a result, the exact velocity distribution, $U_z \equiv \mathrm{Re}\left[U_z^* e^{i\Omega\tau}\right]$, is obtained after the U_z^* is known.

3-5 Concentration Field

The dimensionless governing equation and boundary conditions of the concentration field are:

$$\begin{cases} S_c \dfrac{\partial C_n(R,Z,\tau)}{\partial \tau} + \widetilde{P}_{eD} U_z \dfrac{\partial C_n}{\partial Z} = \dfrac{1}{R}\dfrac{\partial}{\partial R}\left(R\dfrac{\partial C_n}{\partial R}\right) + \dfrac{\partial^2 C_n}{\partial Z^2} \\ \dfrac{\partial C_n(1,Z,\tau)}{\partial R} = 0,\ C_n(0,Z,\tau): \text{finite} \\ \langle C_n(R,0,\tau)\rangle = C_{n,in},\ \langle C_n(R,L/r_0,\tau)\rangle = C_{n,out} \end{cases} \quad (3.1\text{-}19) \sim (3.1\text{-}21)$$

Again, complex variables are used.

Here we focus first on why the two equations, the momentum equation and the concentration equation, are decoupled. In order to solve the concentration, it is assumed that after a long time the concentration is comprised of a linear combination of mean and fluctuating parts. The mean part (steady diffusion) is expected to vary linearly with axial distance [42 ~ 45, 53] and is the solution of

$$\frac{\partial^2 C_{n,steady}}{\partial Z^2} = 0 \quad (3.5\text{-}1)$$

Since the gradient of the concentration along the axial direction is constant, the fluctuation part of the concentration is independent of Z.
With the boundary conditions

$$C_{n,steady}(Z) = C_{n.in} + (C_{n,out} - C_{n,in})\frac{r_0}{L}Z \quad (3.5\text{-}2).$$

Therefore define

$$C_n(R,Z,\tau,\Omega,S_c) = \left[C_{n,in} + (C_{n,out} - C_{n,in})\frac{r_0}{L}Z\right] + \mathrm{Re}\left[C^*_{nR}(R,\Omega,S_c)e^{i\Omega\tau}\right] \quad (3.5\text{-}3)$$

where C_n^* is a complex function.

Substitute above into the dimensionless concentration equation:

$$\begin{cases} (i\Omega)S_c\left(C^*_{nR}e^{i\Omega\tau}\right) + \widetilde{P}_{eD}\left(U^*_z e^{i\Omega\tau}\right)\dfrac{(C_{n,out} - C_{n,in})r_0}{L} = \dfrac{\partial^2 C^*_{nR}}{\partial R^2}e^{i\Omega\tau} + \dfrac{1}{R}\dfrac{\partial C^*_{nR}}{\partial R}e^{i\Omega\tau} \\ \Rightarrow \dfrac{\partial^2 C^*_{nR}}{\partial R^2} + \dfrac{1}{R}\dfrac{\partial C^*_{nR}}{\partial R} - i\Omega S_c C^*_{nR} = \widetilde{P}_{eD}U^*_z C_{ns} \\ \dfrac{\partial C^*_{nR}(1,\Omega)}{\partial R} = 0,\ C^*_{nR}(0,\Omega): \text{finite} \end{cases} \quad (3.5\text{-}4)$$

with $C_{ns} \equiv \dfrac{(C_{n,out} - C_{n,in})r_0}{L}$

It can be seen that the particular solution is this is a non-homogeneous modified Bessel function of zero order with the eiganvalue $\beta_I \equiv \sqrt{i\Omega S_c}$ or $\beta_J \equiv \sqrt{-i\Omega S_c}$.

Then the solution has the form.

$$C^*_{nR} = C_A I_0\left(\sqrt{i\Omega S_c}R\right) + C_B K_0\left(\sqrt{i\Omega S_c}R\right) + C^*_{nR,pt}$$
$$\text{or } = C_A J_0\left(\sqrt{-i\Omega S_c}R\right) + C_B Y_0\left(\sqrt{-i\Omega S_c}R\right) + C^*_{nR,pt}$$
$$\Rightarrow \frac{\partial C^*_{nR}}{\partial R} = C_A\left(\sqrt{i\Omega S_c}\right) I_1\left(\sqrt{i\Omega S_c}R\right) - C_B\left(\sqrt{i\Omega S_c}\right) K_1\left(\sqrt{i\Omega S_c}R\right) + \frac{\partial C^*_{nR,pt}}{\partial R}$$

where C_A and C_B and integral constants.

We find the particular solution is

$$C^*_{nR,pt} = \frac{-iC_{ns}\tilde{P}_{eD}}{(1-S_c)\Omega}\left(U^*_z + \frac{-P^*}{i\Omega S_c} + \frac{-\Psi E^*_z}{K^2 - i\Omega S_c}\right) \qquad (3.5\text{-}5)$$

CHAPTER 4

RESULTS AND PARAMETRIC DISCUSSIONS

In this chapter, the increase of mass transport rate, $\frac{\langle \dot{Q}_{cn} \rangle}{\dot{Q}_{cn,DF}} - 1 \equiv R_Q$, together with the velocity profiles and the concentration distributions are studied parametrically and systematically. The following data are employed for numerical calculations and demonstration of the related transport phenomena.

- $r_0 = 10(\mu m) = 10^{-5}(m)$, $L = 10(cm) = 0.01(m)$
- T = 25° C = 298.15K
- KCl in water $\Rightarrow$ $\begin{cases} z_b = 1, \\ n_b = 1.2\times10^{20}(1/m^3) \Rightarrow c_b = \frac{n_b}{N_A} = 2\times10^{-4}(mol/m^3) \\ \varepsilon_r \cong 78.3 \text{ at } 25°\text{C} \\ \mu_{\text{sloution}} \cong 10^{-3}(N\cdot s/m^2) \Rightarrow \nu_{solution} \cong 10^{-6}(m^2/s) \end{cases}$
- In oreder to obey Debye - Huckle approximation, assume $\frac{z_b e\varphi}{k_b T} = 0.01 \sim 0.05$

  $\varphi = -25\text{mV} \sim -125\text{mV}$
- $E_{zA} = 5\times10^4(V/m) \sim 10^6(V/m)$
- $\frac{(c_{n,out} - c_{n,in})}{L} = -1$, $c_{n,in} = 2\times10^{-4}$

Consequently, the values of the relative dimensionless parameters are $\text{Re} \cong 0.1$, $K \cong 15$, $\Psi_s \cong -1 \sim -5$, $E_z^* \cong 20 \sim 400$, $C_{ns} = -0.001$, and $C_{n,in} = 2$.

Before discussions, the three time constants and the three eiganvalues in the governing equations, which are critical to the transport phenomena, will be stated once more in the following:

$t_\omega \equiv \frac{1}{\omega}$: the time of oscillation,

$t_\nu \equiv \frac{r_0^2}{\nu}$: the response time during which momentum diffuses from the wall of

the tube to the center,

$t_{Dn} \equiv \frac{r_0^2}{D_n}$: the response time during which species n diffuses from the wall of the tube to the center,

K: the thickness of EDL,

Ω: the square of Womersley number,

ΩS_c: the square of Womersley number of diffusion.

4-1 Variations of The Velocity Profiles and The Concentration Distributions

As shown in Fig. 4.1-1, it can be seen that for the flow situation with $S_c = 2$, $\widetilde{P}_{eD} = 0.2$, $K = 15$, $E_z^* = 400$, and $\Psi_s = -5$ the enhancement of the mass transport rate of species n increases first and then decreases with the dimensionless frequency, Ω. The profile indicates a peak value at a specific frequency, i.e., $\Omega_s \cong 4.8$. Such a variation with Ω can be illustrated through the observation of the variations of the velocity profiles and the concentration distributions.

For flow situation with both Ω and ΩS_c smaller, e.g., Ω=0.25 in Fig. 4.1-4, the relationship of the three time constants is $t_\nu < t_{Dn} < t_\omega$.Physically, it means the momentum and mass diffusions are fast then the variation of the electrical field. The velocity and concentration profiles remain almost uniform across the micro-tube, resulting therefore a negligibly small increase of mass transport rate due to the oscillating flow motion. , resulting a larger concentration gradient and thus a larger mass diffusion near the boundary.

As Ω increase such that $t_\nu < t_\omega < t_{Dn}$, e.g., Ω=0.75 in Fig. 4.1-5, the fluid particles still have enough time to diffuse momentum from the boundary to the central region, but the diffusion of species n does not. Consequently, the mass transport rate increases.

When Ω is greater than unity so that: $t_\omega < t_\nu < t_{Dn}$, both the fluid particles and species n do not have enough time to diffuse momentum and mass from the boundary to the center. Thus the velocity profile becomes concave form at center, i.e., the flow is slower at center, as shown in Fig. 4.1-3. A radial concentration gradient is also formed near the boundary and leads a diffusion of species n toward the center. That is, the diffusion is from a region with a higher velocity and near the boundary to a region with lower velocity and concentration at the center, resulting an increasing of R_Q.

As Ω keeps increasing, e.g., Ω=10 as shown in Fig. 4.1-7, the flow direction in the central portion might be opposite to that near the boundary during the periodic

motion. The enhancement of the mass transport rate due to the oscillating EOF is thus suppressed and even reduced, resulting a peak value at a certain specific Ω. When Ω becomes even large, e.g., Ω=100 in Fig. 4.1-11, the velocity at the center portion remains nearly quiaescent and the concentration distribution therein does not vary with the flow. The effects of EDL on the velocity and concentration distributions are then limited to a region close to the boundary. The time-averaged mass flow rate is therefore not enhanced by the flow.

CHAPTER 5

CONCLUSIONS AND FUTURE WORK

5-1 Conclusions

A time periodic electroosmotic flow has been used to drive the flow in micropipette. The phenomenon of electrical double layer was investigated and the theory of Taylor dispersion was studied. The complex variable approach has been applied to attain the velocity profile, the concentration distribution and the mass flow rate in a micropipette driven by an oscillating EOF.

It was demonstrated that the enhancement of the mass transport rate, $\frac{\langle \dot{Q}_{cn} \rangle}{\dot{Q}_{cn,DF}} - 1 \equiv R_Q$, increases first and then decreases with the frequency of the electrical field applied. Parametric studies uncovered that the three time constants, $t_\omega \equiv \frac{1}{\omega}$, $t_\nu \equiv \frac{r_0^2}{\nu}$, and $t_{Dn} \equiv \frac{r_0^2}{D_n}$ together with the three eiganvalues in the three governing equations Ω, ΩS_c, and K played significant roles in the process of mass transport.

The results indicates that the velocity profile, the concentration distribution , and, consequently, the mass transport rate, R_Q, depends significantly on Ω and ΩS_c. The Schmidt number, S_c, and the thickness of EDL, K also affect the variation of R_Q. Furthermore, it has been shown that at low frequency the oscillating EOF is conducive to the separation of species.

5-2 Future Work

The model of this study is restricted to the flow region with in small Reynolds numbers, and small electrical potential on the surface of the tube. It can be extended by removing these restrictions to study the effects of inertial effects on mass transport. Moreover, the effect of heterogeneity with non-uniform zeta potential is also very interesting and important in the species mixing. Numerical simulation may then be needed to study such a transport phenomenon.

Reference

[1] J. Young, "Lab On A Chip," *Forbes*, **Vol. 158**, No. 7, pp. 210-211, 1996

[2] M. Kuschel, "Lab-On-A-Chip Technology - Applications for The Life Sciences," *Biofarm*, **Vol. 14**, No. 8, pp. 50-52, 2001

[3] G. Ondrey, "The 'Lab-On-A-Chip' Isn't Science Fiction Anymore," Chem. Eng., **Vol. 104**, No. 4, pp. 48-&, 1997

[4] J. G. E. Gardeniers, A. van den Berg, "Lab-On-A-Chip Systems for Biomedical and Environmental Monitoring," *Fresenius' J. Anal. Chem.*, **Vol. 378**, No. 7, pp. 1700-1703, 2004

[5] U. J. Krull, "Special Issue: Microfluidics and Lab-On-A-Chip – Foreword," *Anal. Chim. Acta*, **Vol. 507**, No. 1, pp. 1-1, 2004

[6] R. J. Hunter, "*Zeta Potential in Colloid Science: Principles and Applications*," London ; New York : Academic Press, 1981

[7] R. F. Probstein, "*Physicochemical Hydrodynamics: an Introduction, 2nd ed.*," New York : John Wiley & Sons, 1994

[8] J. S. Newman, "*Electrochemical System, 2nd ed.*," Englewood Cliffs, N. J. : Prentice Hall, 1991

[9] M. J. Clifton, "Numerical-Simulation of Protein Separation by Continuous-Flow Electrophoresis," *Electrophoresis*, **Vol. 14**, No. 12, pp. 1284-1291, 1993

[10] L. Hu, J. D. Harrison, and J. H. Masliyah, "Numerical Model of Electrokinetic Flow for Capillary Electrophoresis," *J. Colloid Interface Sci.*, **Vol. 215**, No. 2, pp. 300-312, 1999

[11] G. I. Taylor," Dispersion of Soluble Matter in Solvent Flowing Slowly Through a Tube," *Proc. R. Soc. London, Ser. A*, **Vol. 219**, pp. 186-203, 1953

[12] G. I. Taylor," The Dispersion of Matter in Turbulent Flow Through a Pipe," *Proc. R. Soc. London, Ser. A*, **Vol. 223**, pp. 446-468, 1954

[13] G. I. Taylor," Conditions Under Which Dispersion of a Solute in a Stream of Solvent Can be Used to Measure Molecular Diffusion," *Proc. R. Soc. London, Ser. A*, **Vol. 223**, pp. 473-477, 1954

[14] R. Aris, "On The Dispersion of Solute in a Fluid Flowing Through a Tube," *Proc. R. Soc. London, Ser. A*, **Vol. 235**, pp. 67-77, 1956

[15] W. H. Lim, H. M. Jang, S. M. Ha, Y. G. Chai, S. I. Yoo, and B. T. Zhang, "A Lab-On-A-Chip Module for Bead Separation in DNA-Based Concept Learning," *DNA computing : 9th International Workshop on DNA Based Computers*, **Vol. 2943**, pp. 1-9, 2004

[16] M. Krishnan, V. Namasivayam, R. S. Lin, R. Pal, and M. A. Burns,

"Microfabricated Reaction and Separation Systems," *Current Opinion in Biotechnology* , **Vol. 12**, No. 1, pp. 92-98, 2001

[17] A. K. Jain and R. K. Srivastava, "Ab-Initio Studies on Electroosmotic Separation: Separation of 1,4-Dioxane in Water Solution," *J. Membr. Sci.*, **Vol. 112**, No. 1, pp. 41-46, 1996

[18] J. C. T. Eijkel, A. van den Berg, A. Manz, "Cyclic Electrophoretic and Chromatographic Separation Methods," *Electrophoresis*, **Vol. 25**, No. 2, pp. 243-252, 2004

[19] K. D. Bartle and P. Myers, "Theory of Capillary Electrochromatograpy," *Journal of Chromatography. A,* **Vol. 916**, No. 1-2, pp. 3-23, 2001

[20] G. M. Mala, D. Li, and J. D. Dale, "Heat Transfer and Fluid Flow in Microchannels," *Int. J. Heat Transfer*, **Vol. 40**, No. 13, pp. 3079-3008, 1997

[21]G. M. Mala, D. Li, C. Werner, H. J. Jacobasch, Y. B. Ning, "Flow Characteristics of Water Through a Microchannel Between Two Parallel Plates with Electrokinetic Effects," *Int. J. Heat and Fluid Flow*, **Vol. 18**, No. 5, pp. 489-496, 1997

[22] C. Yang, D. Li, and J. H. Masliyah, "Modeling Forced Liquid Convection in Rectangular Microchannels with Electrokinetic Effects," *Int. J. Heat Mass Transfer*, **Vol. 41**, No. 24, pp. 4229-4249, 1998

[23] R. J. Yang, L. M. Fu, and Y. C. Lin, "Electroosmotic Flow in Microchannels," *J. Colloid Interface Sci.*, **Vol. 239**, No. 1, pp. 98-105, 2001

[24] R. J. Yang, L. M. Fu, and C. C. Hwang, "Electroosmotic Entry Flow in a Microchannel," *J. Colloid Interface Sci.*, **Vol. 244**, No 1, pp. 173-179, 2001

[25] J. G. Santiago, "Electroosmotic Flows in Microchannels with Finite Inertial and Pressure Forces," *Anal. Chem.*, **Vol. 73**, No. 10, pp. 2353-2365, 2001

[26] A. D. Stroock, M. Weck, D. T. Chiu, W. T. S. Huck, P. J. A. Kenis, R. F. Ismaglilov, and G. M. Whitesides, "Patterning Electro-osmotic Flow with Patterned Surface Charge," *Phys. Rev. Lett.*, **Vol. 84**, No. 15, pp. 3314-3317, 2000

[27] L. Ren and D. Li, "Electroosmotic Flow in Heterogeneous Microchannels," *J. Colloid Interface Sci.*, **Vol.** 243, No. 1, pp. 255-261, 2001

[28] L. Ren, C. Escobedo, and D. Li, "Electroosmotic Flow in a Microcapillary with One Solution Displacing Another Solution," *J. Colloid Interface Sci.*, **Vol. 242**, No. 1, pp. 264-271, 2001

[29] D. Erickson and D. Li, "Influence of Surface Heterogeneity on Electrokinetically Driven Microfluidic Mixing," *Langmuir*, **Vol.** 18, No. 5, pp. 1883-1892, 2002

[30] J. P. Gleeson, "Electroosmotic Flows with Random Zeta Potential," *J. Colloid Interface Sci.*, **Vol. 249**, No. 1, pp. 217-226, 2002

[31] O. Söderman and B. Jönsson, "Electro-osmosis Velocity Profiles in Different Geometries with Both Temporal and Spatial Resolution," *J. Chem. Phys.*, **Vol. 105**, No. 23, pp. 10300-10311, 1996

[32] N. G. Green, A. Ramos, A. Gonzalez, H. Morgan, and A. Castellanos, "Fluid Flow Induced by Nonuniform AC Electric Fields in Electrolytes on Microelectrodes I. Experimental Measurements," *Physical Review E*, **Vol. 61**, No. 4, pp. 4011-4018, Part B, 2000

[33] A. Gonzalez, A. Ramos, N. G. Green, A. Castellanos, and H. Morgan, "Fluid Flow Induced by Nonuniform AC Electric Fields in Electrolytes on Microelectrodes II. A Linear Double-Layer Analysis," *Physical Review E*, **Vol. 61**, No. 4, pp. 4019-4028, Part B, 2000

[34] P. Dutta, and A. Beskok, "Analytical Solution of Time Periodic Electroosmotic Flows: Analogies to Stokes' Second Problem," *Anal. Chem.*, **Vol. 73**, No. 21, pp. 5097-5102, 2001

[35] D. Erickson and D. Li, "Analysis of Alternating Current Electroosmotic Flows in a Rectangular Microchannel," *Langmuir*, **Vol. 19**, No. 13, pp. 5421-5430, 2003

[36] A. Bhattacharyya and J. H. Masliyah, and J. Yang, "Oscillating Laminar Electrokinetic Flow in Infinitely Extended Circular Microchannels," *J. Colloid Interface Sci.*, **Vol. 261**, No. 1, pp. 12-20, 2003

[37] A. R. Mansour, "Dispersion of Solute in Laminar – Flow Through a Circular Tube," *Sep. Sci.Technol.*, **Vol. 24**, No. 15, pp. 1437-1442, 1989

[38] M. Martin and G. Guiochon, "Axial Dispersion in Open-Tubular Capillary Liquid Chromatography with Electroosmotic Flow," *Anal. Chem.*, **Vol. 56**, No.4, pp. 614-620, 1984

[39] J. P. McEldoon and R. Datta, "Analytical Solution for Dispersion in Capillary Liquid Chromatography with Electroosmotic Flow," *Anal. Chem.*, **Vol. 64**, No.2, pp. 227-230, 1992

[40] S. K. Griffiths and R. H. Nilson, "Hydrodynamic Dispersion of a Neutral Nonreacting Solute in Electroosmotic Flow," *Anal. Chem.*, **Vol. 71**, No.24, pp. 5522-5529, 1999

[41] S. K. Griffiths and R. H. Nilson, "Electroosmotic Fluid Motion and Late-Time Solute Transport for Large Zeta Potentials," *Anal. Chem.*, **Vol. 72**, No.20, pp. 4767-4777, 2000

[42] H. Harris and S. Goren, " Axial Diffusion in a Cylinder with Pulsed Flow," *Chem. Eng. Sci.*, **Vol. 22**, pp. 1571-1576, 1967

[43] R. G. Rice and L. C. Eagleton, "Mass Transfer Produced by Laminar Flow Oscillations," *Can. J. Chem. Eng.*, **Vol. 48**, pp. 46-51,1970

[44] P. C. Chatwin, "On The Longitudinal Dispersion of Passive Contaminant in

Oscillatory Flows in Tubes," *J. Fluid Mech.*, part3, **Vol. 71**, pp. 513-527, 1975

[45] E. J. Watson, "Diffusion in Oscillatory Pipe Flow," *J. Fluid Mech.*, **Vol. 133**, pp. 233-244, 1983

[46] P. E. Hydon and T. J. Pedley, "Axial –Dispersion in a Channel with Oscillating Walls," *J. Fluid Mech.*, **Vol. 249**, pp. 535-555, 1993

[47] U. H. Kurzweg and M. J. Jaeger, "Diffusional Separation of Gases by Sinusoidal Oscillations," *Phys. Fluids*, **Vol. 30**, No.4, pp. 1023-1025, 1987

[48] U. H. Kurzweg, "Enhanced Diffusional Separation in Liquids by Sinusoidal Oscillations," *Sep. Sci.Technol.*, **Vol. 23**, No.1-3, pp. 105-117,1988

[49] M. J. Jaeger, P. Kalle, and U. H. Kurzweg, "Separation of Gases by Enhanced Upstream Diffusion," *Sep. Sci.Technol.*, **Vol. 27**, No. 6, pp. 691-702,1992

[50] M. J. Jaeger, "The Enrichment of the Heavier of Two Gases Isotopes by Enhanced Diffusion (example H2^2/H2^1)," *Sep. Sci.Technol.*, **Vol. 31**, No. 6, pp. 811-827, 1996

[51] M. J. Jaeger, "The Enrichment of the Lighter of Two Gases by Enhanced Diffusion (example He/N2)," *Sep. Sci.Technol.*, **Vol. 31**, No. 7, pp. 987-992,1996

[52] J. G. Zhang , W. C. Zegel, and U. H. Kurzweg, "Enhanced Axial Dispersion in Oscillating Pipe Flow with Different Solute Concentrations at Its Ends," *J. Fluid Eng.*, **Vol. 118**, No. 1, pp. 160-165, 1996

[53] A. M. Thomas and R. Narayanan, "Physics of OscillatoryFlow and Its Effect on The Mass Transfer and Separation of Species," *Physics of Fluids*, **Vol. 13**, No. 4, pp. 859-866, 2001

[54] A. M. Thomas and R. Narayanan, "A Comparison Between The Enhanced Mass Transfer in Boundary and Pressure Driven Oscillatory Flow," *Int. J. Heat Mass Transfer*, **Vol. 45**, No. 19, pp. 4057-4062, 2002

[55] S. Uchida, "The Pulsating Viscous Flow on the Steady Laminar Motion of Incompressible Fluid in a Circular Pipe," *ZAMP*, pp. 403, 1950

[56] D. K. Cheng, "*Field and Wave Electromagnetics, 2nd ed.*," Reading, Mass. : Addison-Wesley Pub. Co., 1989

[57] Ph. W. M. Rutten, "*Diffusion in Liquids*," Delft : Delft University Press, 1992

[58] Bateman Manuscript Project, "*Higher Transcendental Functions*," New York : McGraw-Hill, 1953-55

[59] N.W. McLachlan, "*Bessel Functions for Engineers*," London, Geoffrey Cumberlege, Oxford Univ. press, 1948

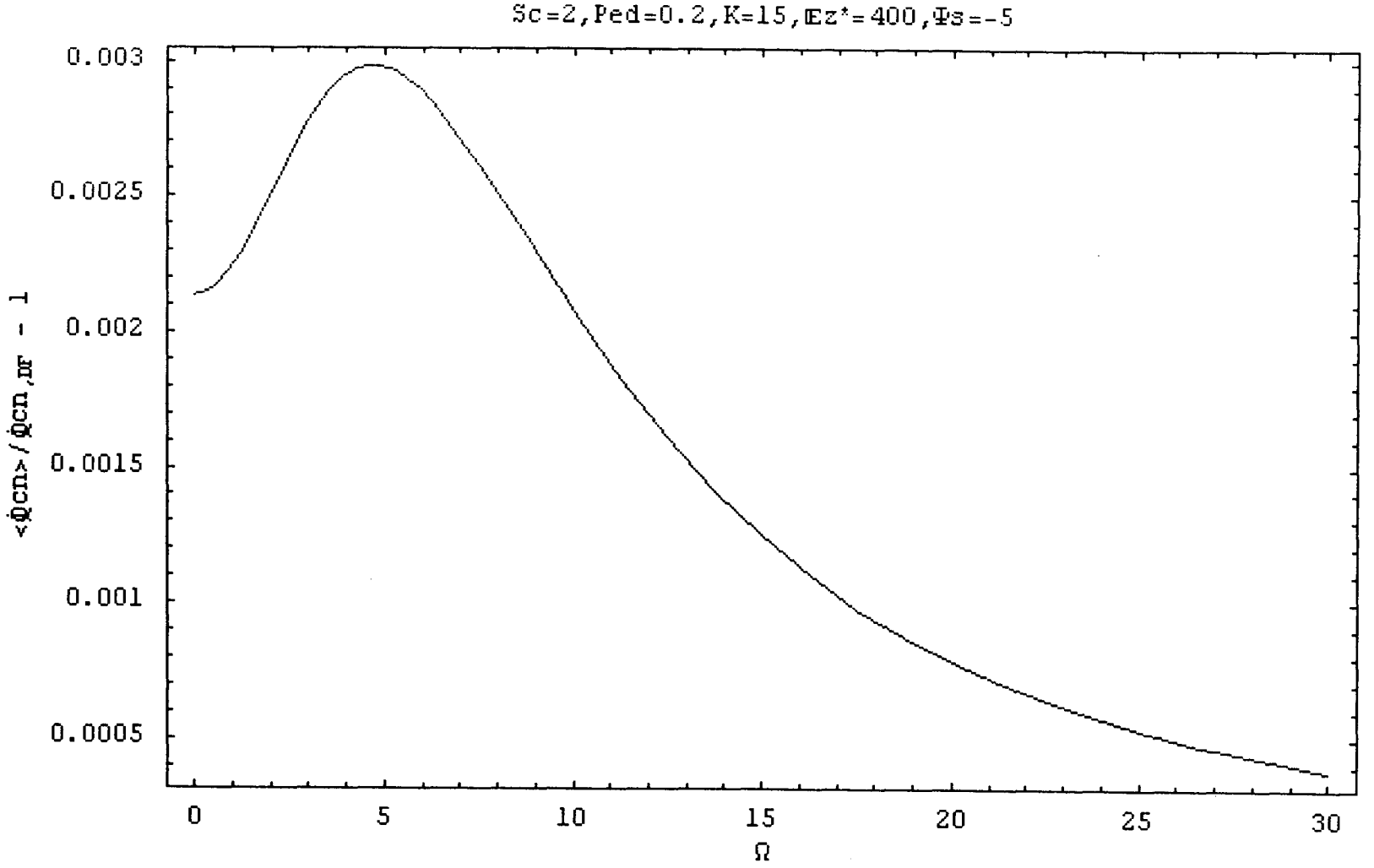

Fig. 4.1-1 The dependence of the increase of mass transfer rate on variation of the dimensionless frequency at $S_c = 2$, $\tilde{P}_{eD} = 0.2$, $K = 15$, $E_z^* = 400$, and $\Psi_s = -5$

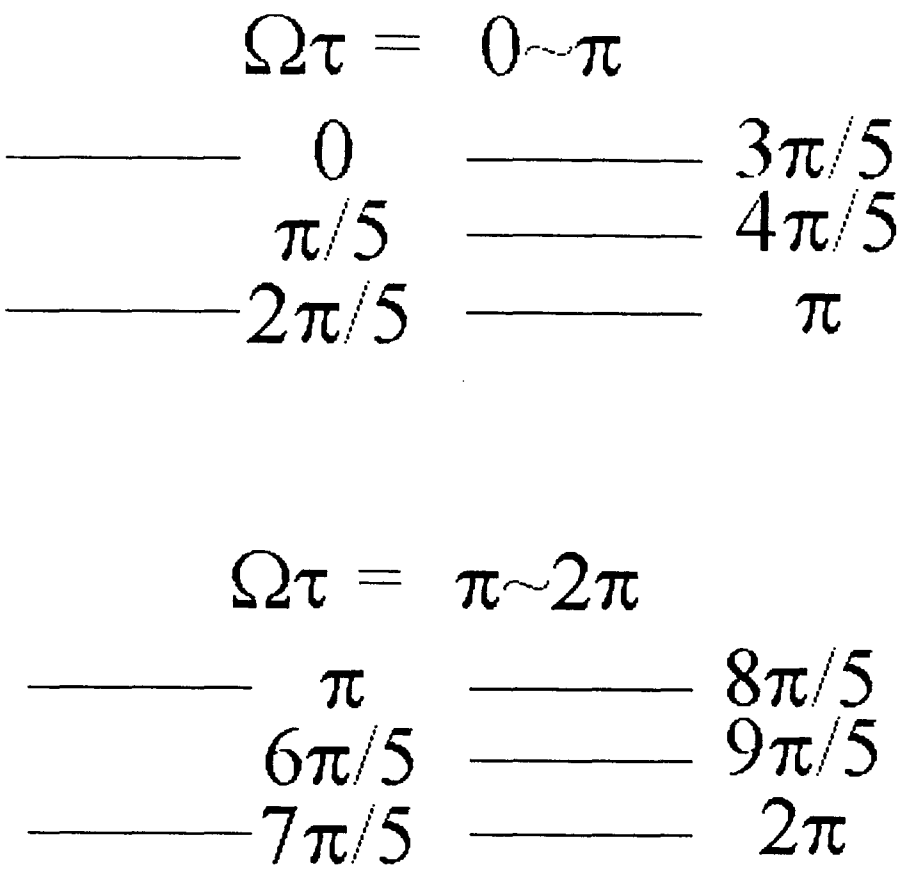

Fig. 4.1-2 Color lines representing the velocity profile or concentration distribution at $\Omega\tau = 0 \sim 2\pi$. (a) $\Omega\tau = 0 \sim \pi$ (b) $\Omega\tau = \pi \sim 2\pi$

Ω =4.8

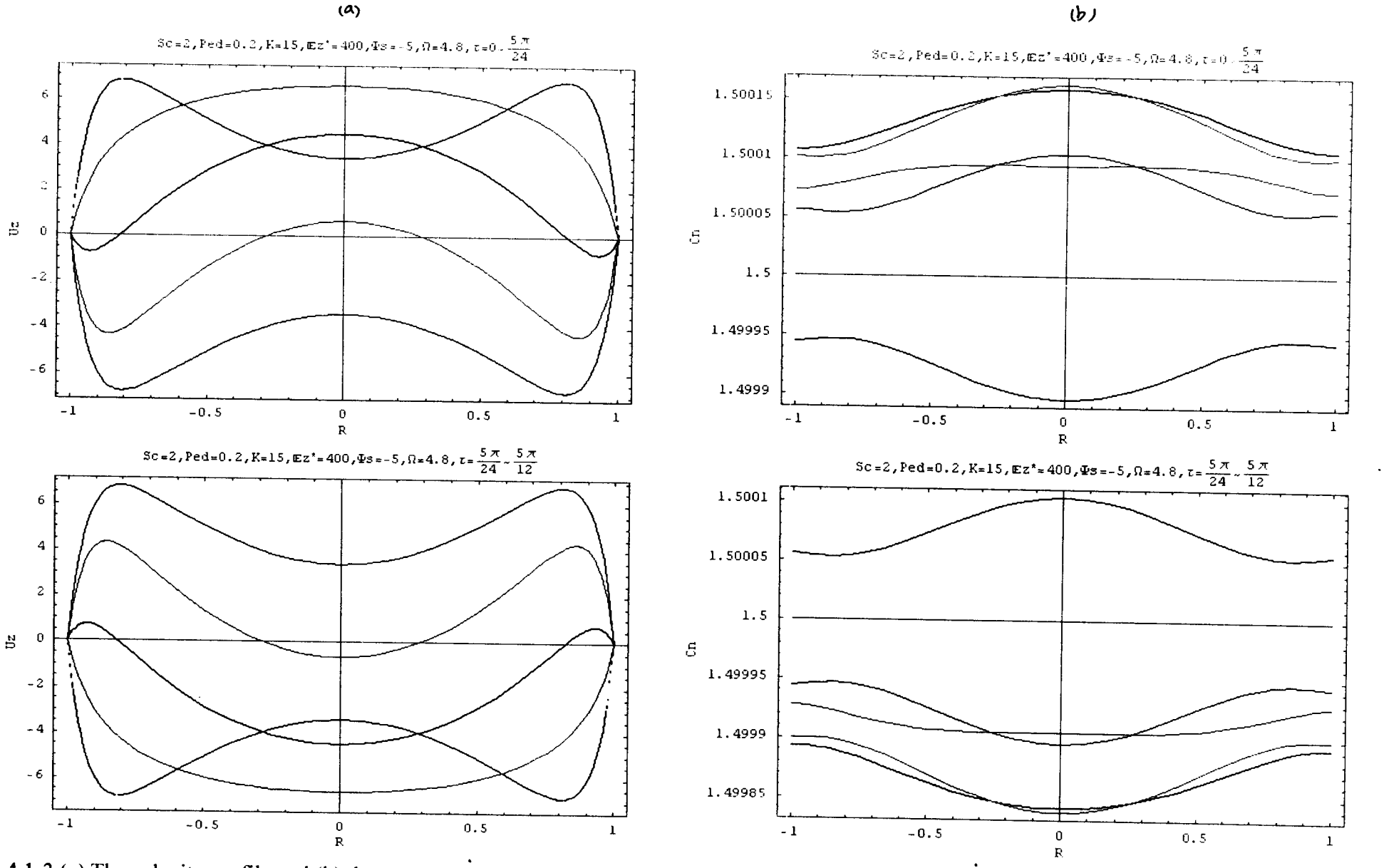

Fig. 4.1-3 (a) The velocity profile and (b) the concentration profile in the microtube at $Z = 500$, $S_c = 2$, $\tilde{\tilde{P}}_{eD} = 0.2$, $K = 15$, $E_z^* = 400$, and $\Psi_s = -5$, under the dimensionless frequency $\Omega = 4.8$ during $\Omega\tau = 0 \sim 2\pi$

Ω = 0.25

(a)

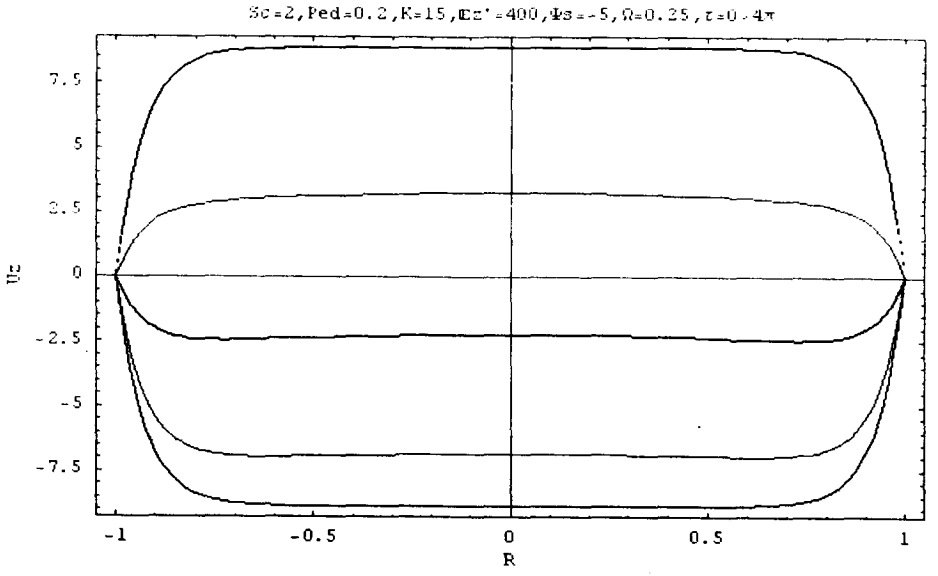

(b)

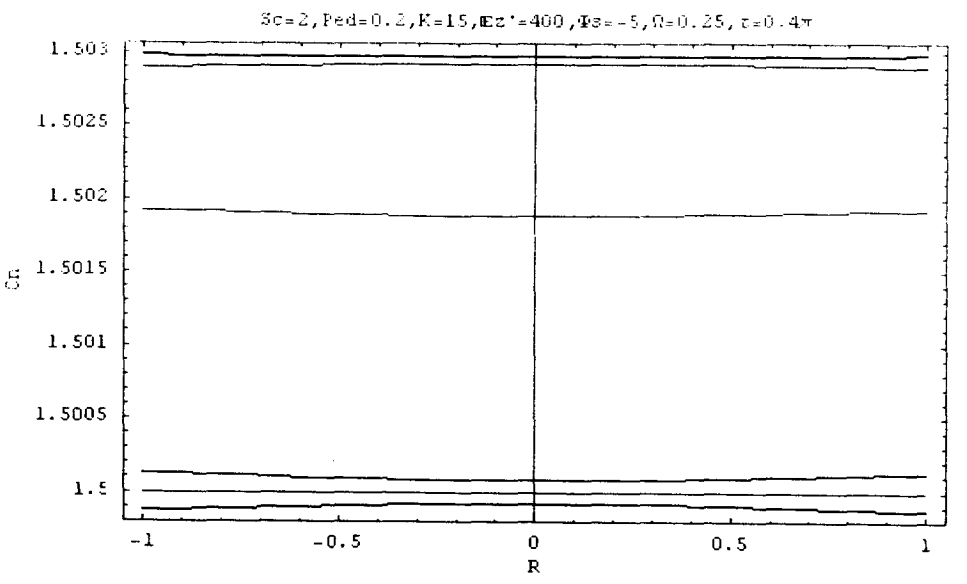

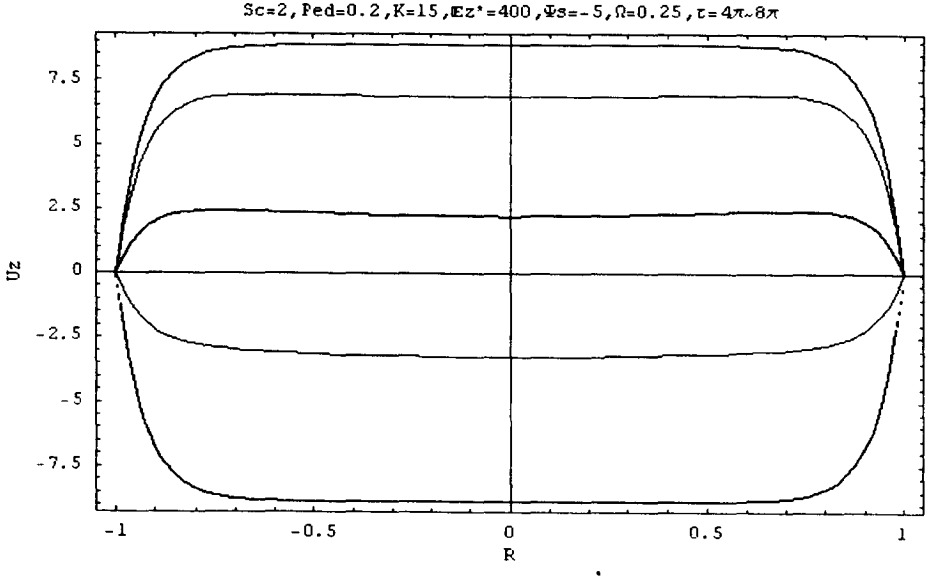

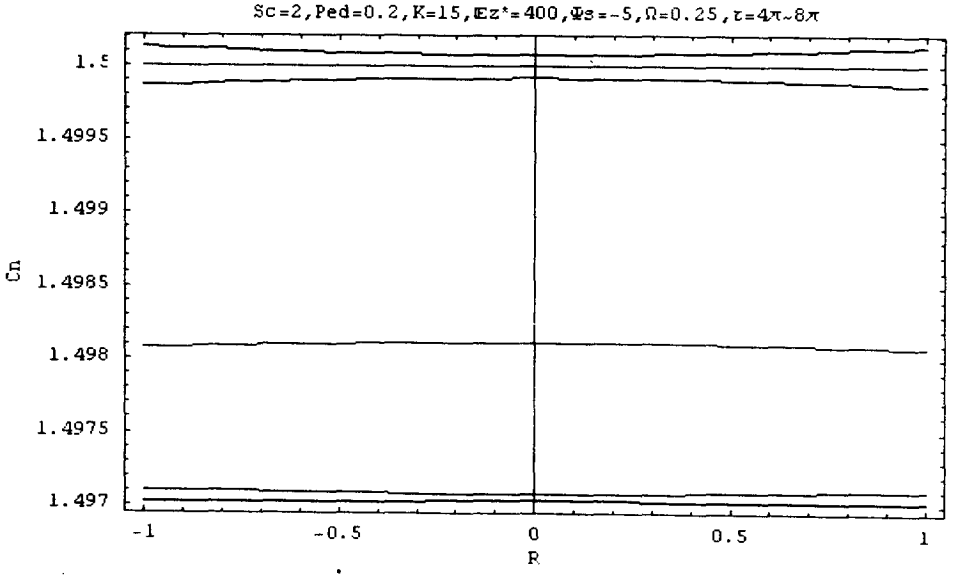

Fig. 4.1-4 (a) The velocity profile and (b) the concentration profile in the microtube at $Z = 500$, $S_c = 2$, $\tilde{P}_{eD} = 0.2$, $K = 15$, $E_z^* = 400$, and $\Psi_s = -5$, under the dimensionless frequency $\Omega = 0.25$ during $\Omega\tau = 0 \sim 2\pi$

Ω=0.75

(a)

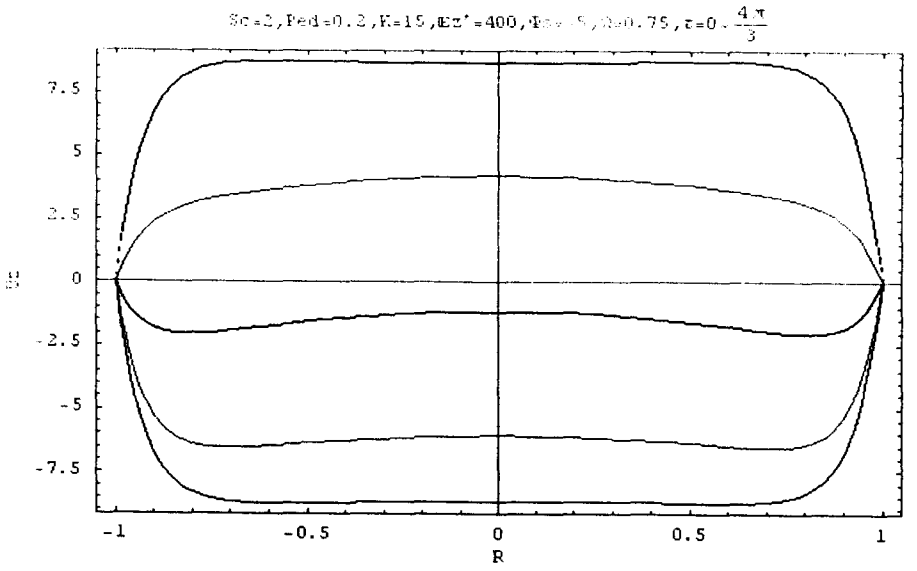

(b)

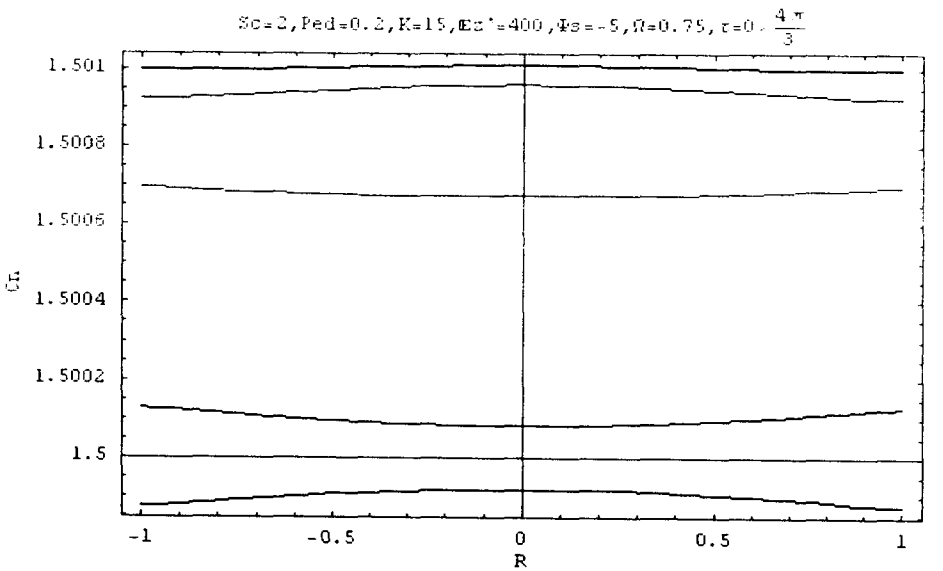

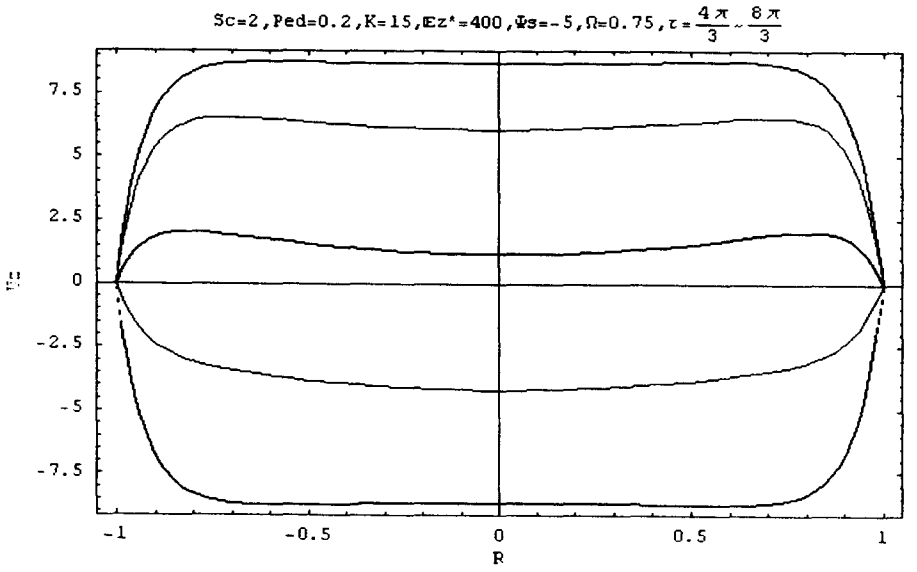

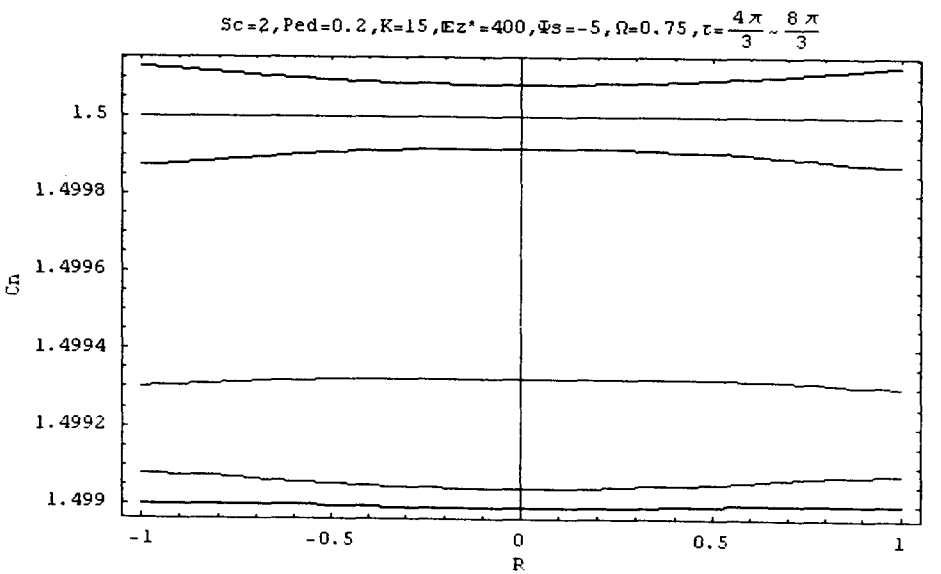

Fig. 4.1-5 (a) The velocity profile and (b) the concentration profile in the microtube at $Z = 500$, $S_c = 2$, $\tilde{P}_{eD} = 0.2$, $K = 15$, $E_z^* = 400$, and $\Psi_s = -5$, under the dimensionless frequency $\Omega = 0.75$ during $\Omega\tau = 0 \sim 2\pi$

Ω=1

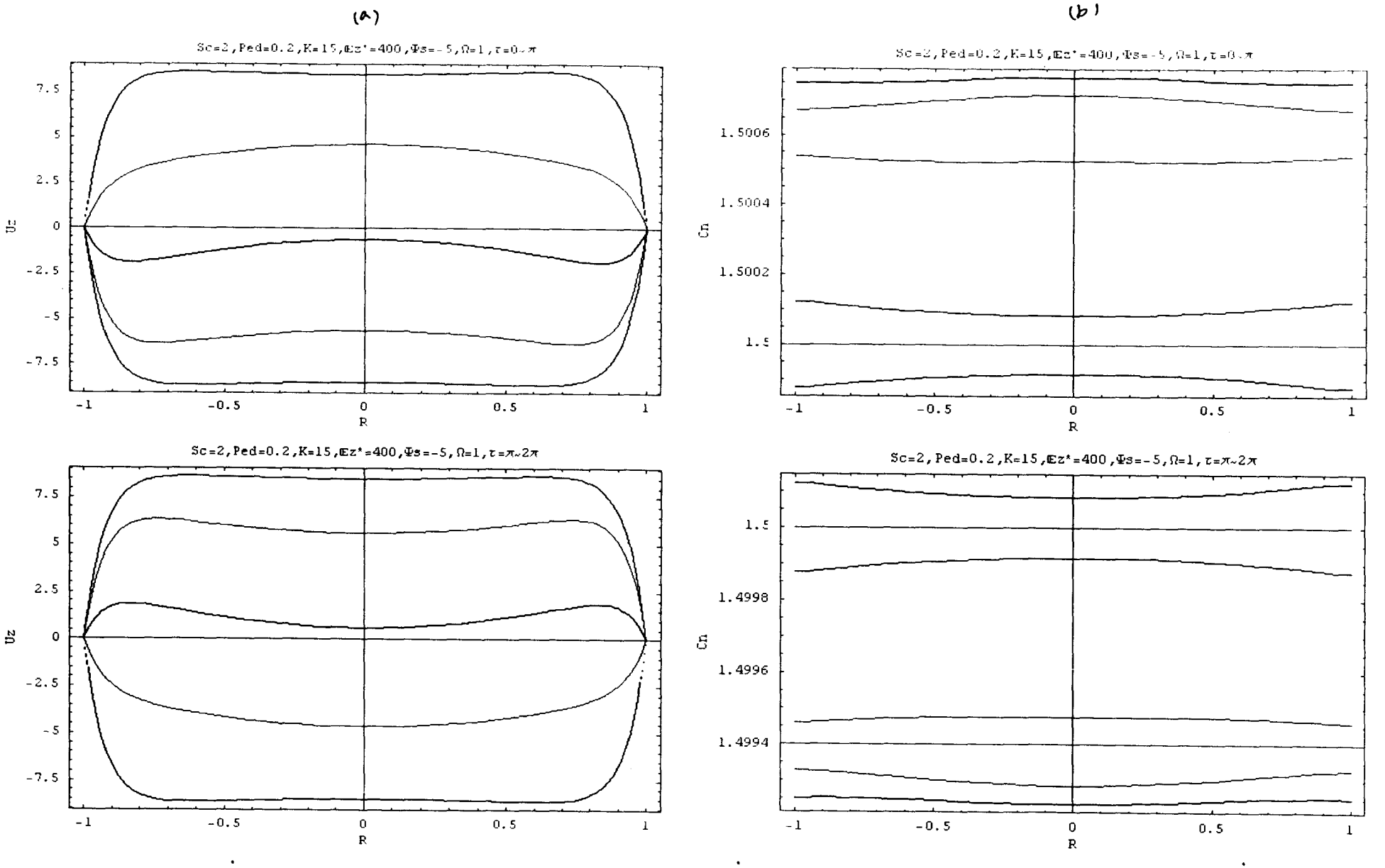

Fig. 4.1-6 (a) The velocity profile and (b) the concentration profile in the microtube at $Z = 500$, $S_c = 2$, $\widetilde{P}_{eD} = 0.2$, $K = 15$, $E_z^* = 400$, and $\Psi_s = -5$, under the dimensionless frequency $\Omega = 1$ during $\Omega\tau = 0 \sim 2\pi$

Ω=10

(a)

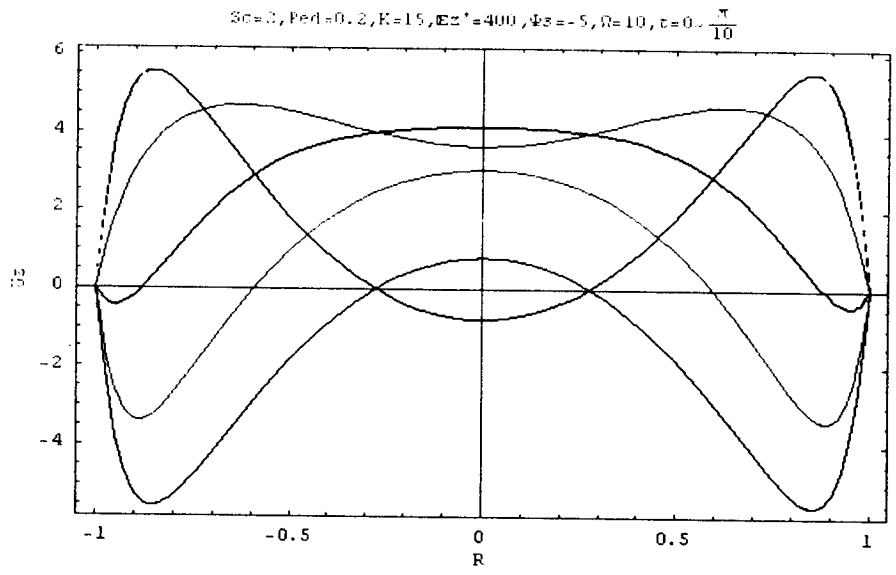

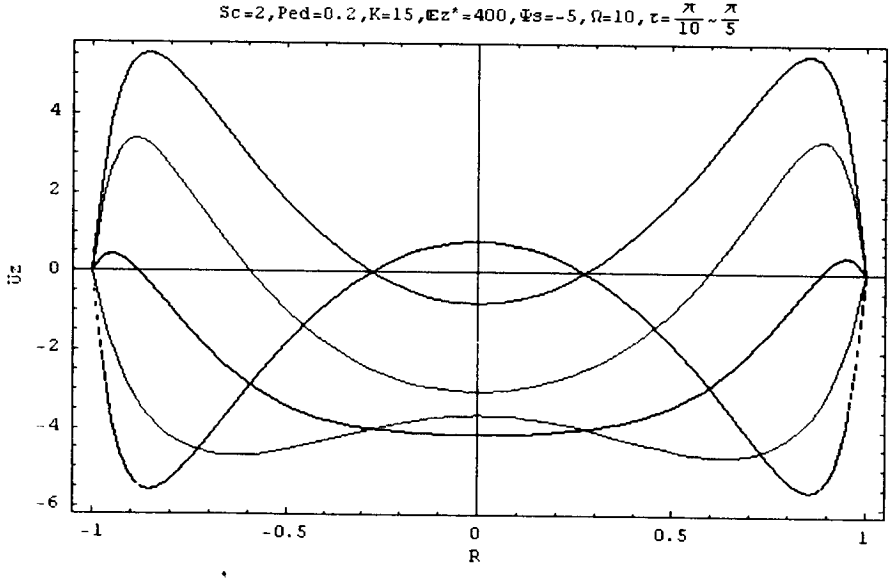

(b)

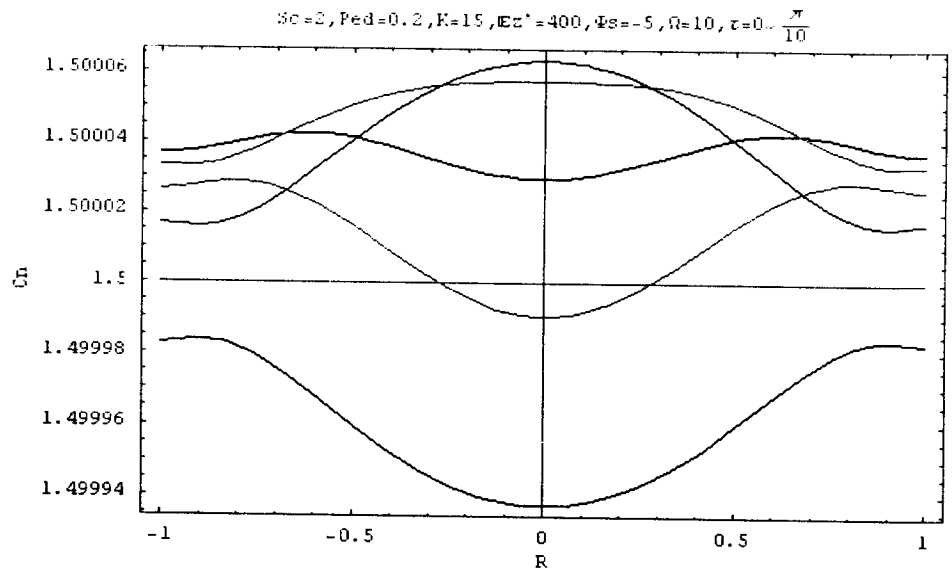

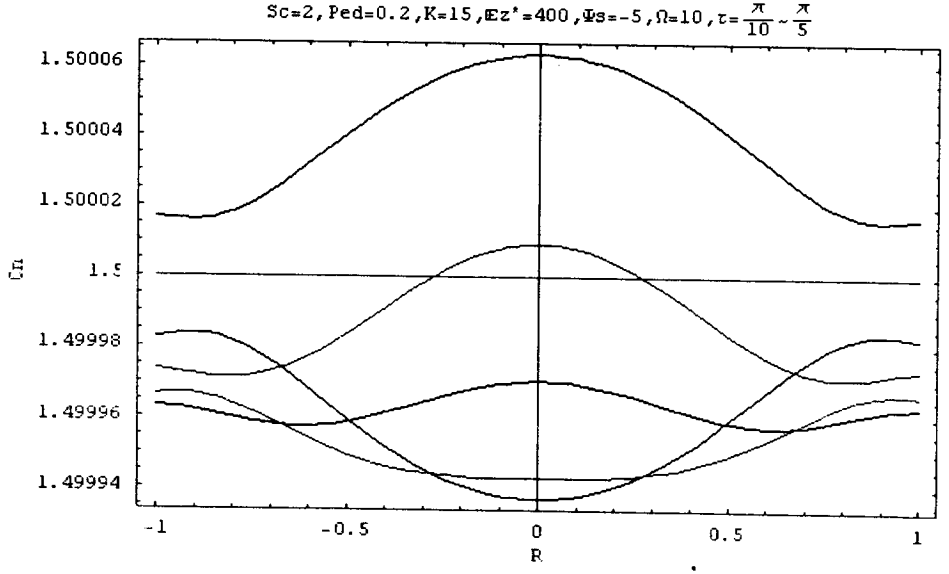

Fig. 4.1-7 (a) The velocity profile and (b) the concentration profile in the microtube at $Z = 500$, $S_c = 2$, $\tilde{P}_{eD} = 0.2$, $K = 15$, $E_z^* = 400$, and $\Psi_s = -5$, under the dimensionless frequency $\Omega = 10$ during $\Omega\tau = 0 \sim 2\pi$

Ω=15

(a)

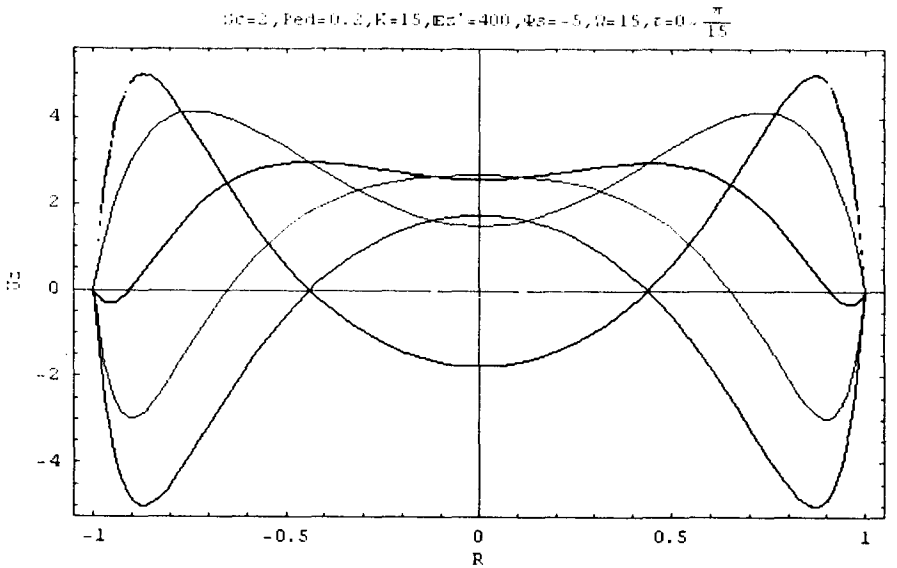

(b)

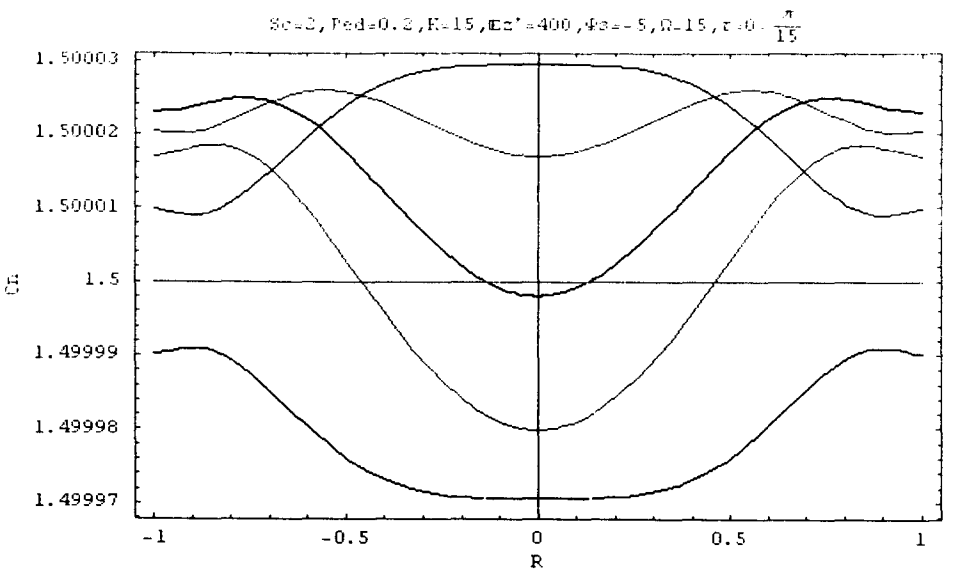

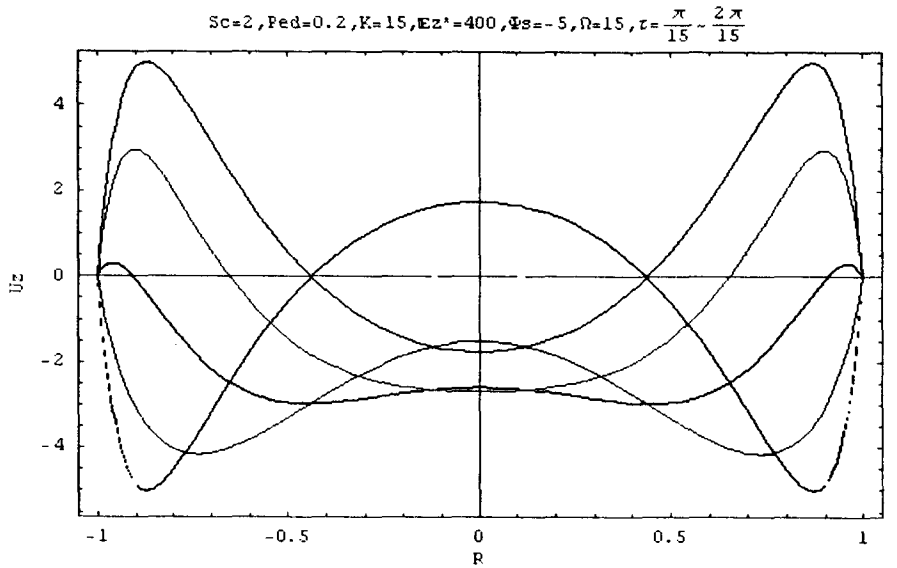

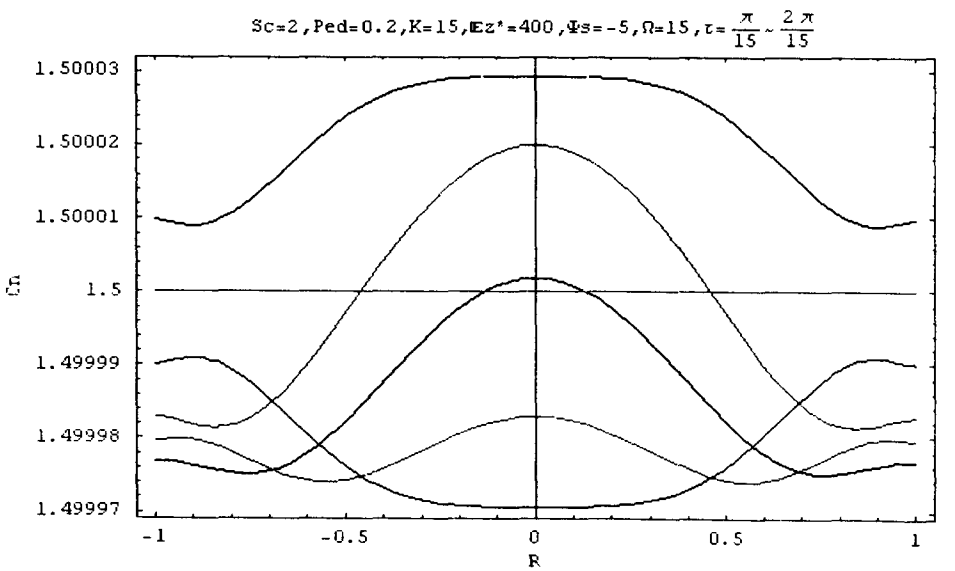

Fig. 4.1-8 (a) The velocity profile and (b) the concentration profile in the microtube at $Z = 500$, $S_c = 2$, $\tilde{P}_{eD} = 0.2$, $K = 15$, $E_z^* = 400$, and $\Psi_s = -5$, under the dimensionless frequency $\Omega = 15$ during $\Omega\tau = 0 \sim 2\pi$

Ω=30

(a)

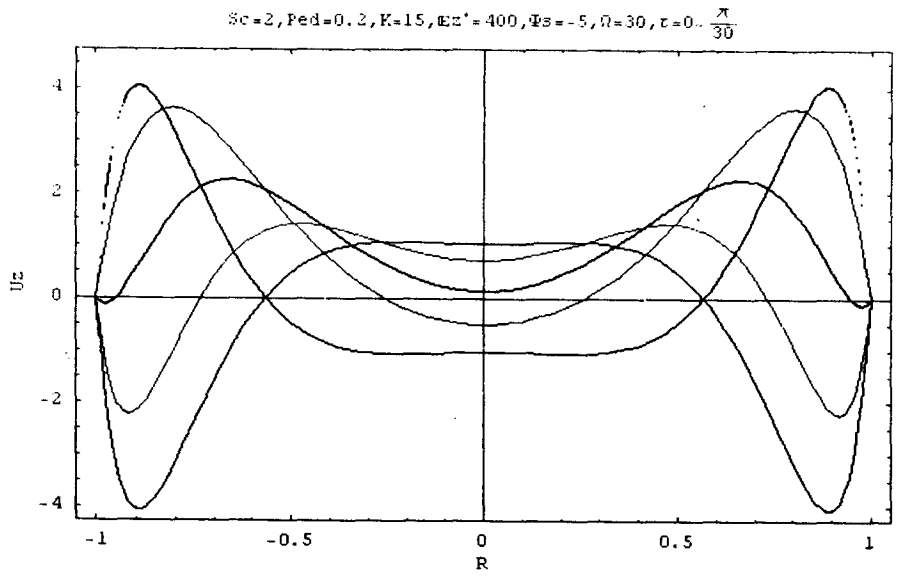

(b)

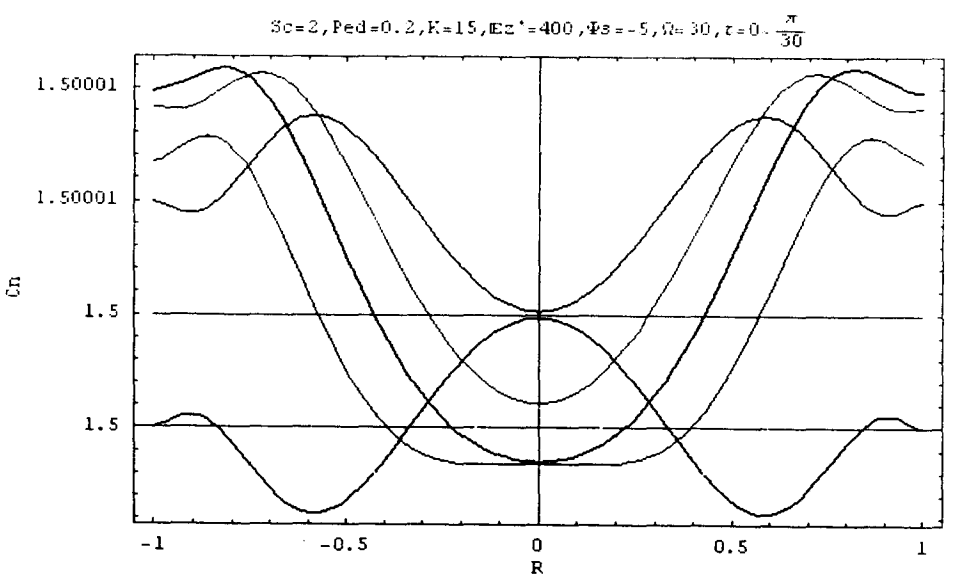

(c)

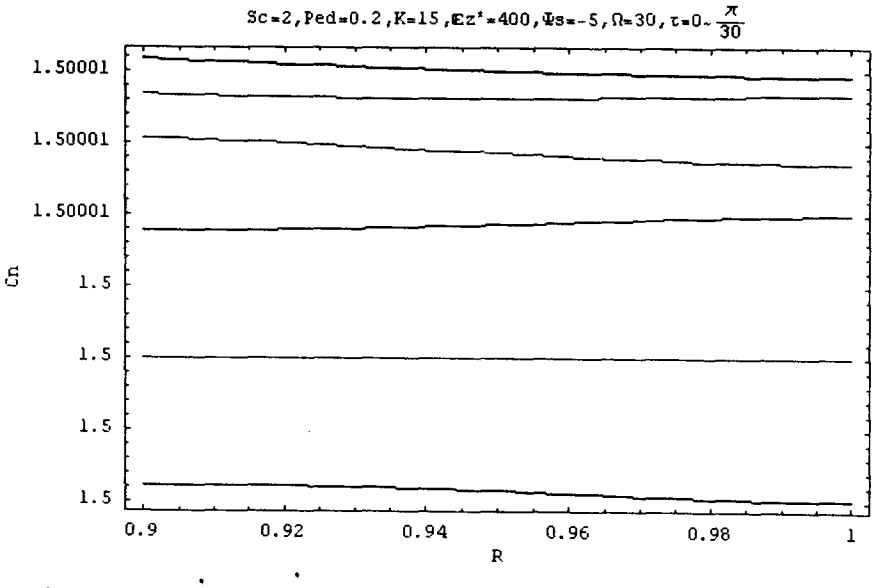

Fig. 4.1-9 (a) The velocity profile, (b) the concentration profile, and (c) the concentration profile between $r = 0.9 \sim 1$ in the microtube at $Z = 500$, $S_c = 2$, $\widetilde{P}_{eD} = 0.2$, $K = 15$, $E_z^* = 400$, and $\Psi_s = -5$, under the dimensionless frequency $\Omega = 30$ during $\Omega\tau = 0 \sim \pi$

Ω=50

(a)

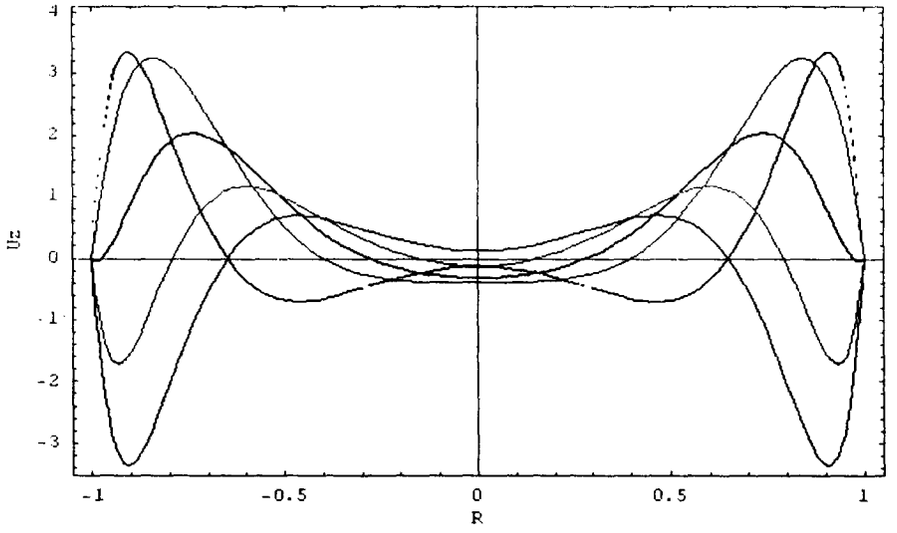

(b)

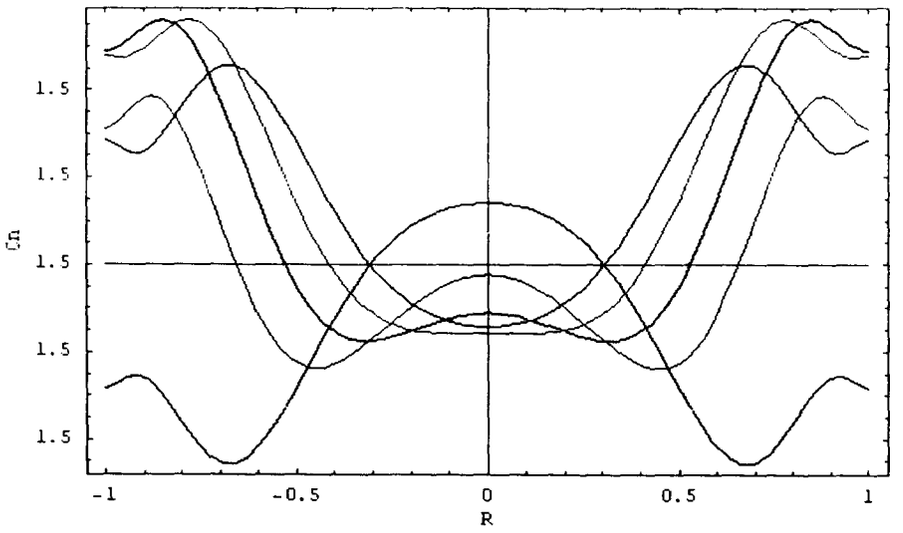

(c)

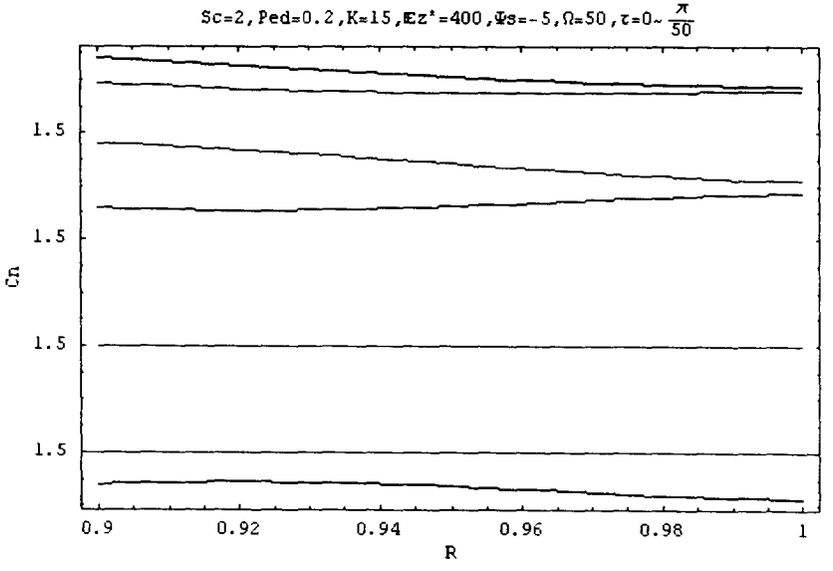

Fig. 4.1-10 (a) The velocity profile, (b) the concentration profile, and (c) the concentration profile between $r = 0.9 \sim 1$ in the microtube at $Z = 500$, $S_c = 2$, $\widetilde{P}_{eD} = 0.2$, $K = 15$, $E_z^* = 400$, and $\Psi_s = -5$, under the dimensionless frequency $\Omega = 50$ during $\Omega\tau = 0 \sim \pi$

Ω=100

(a)

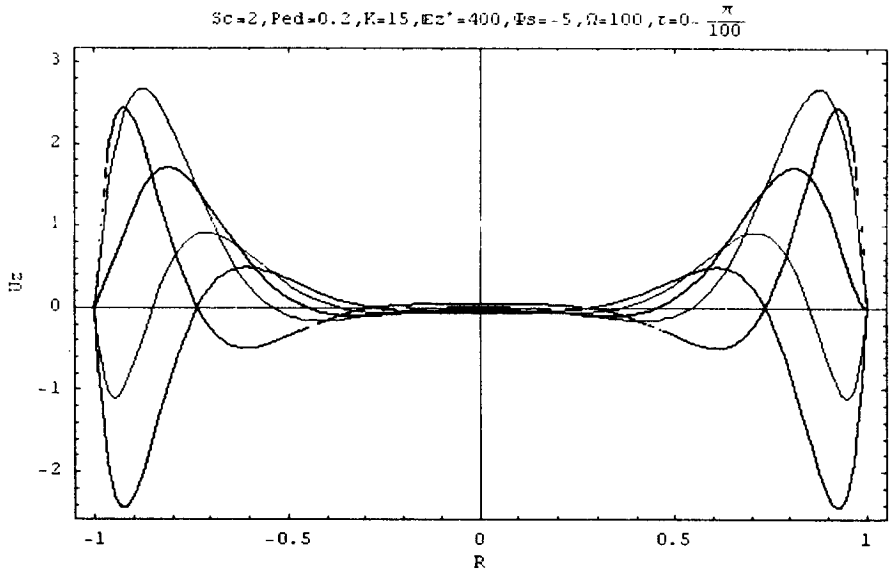

(b)

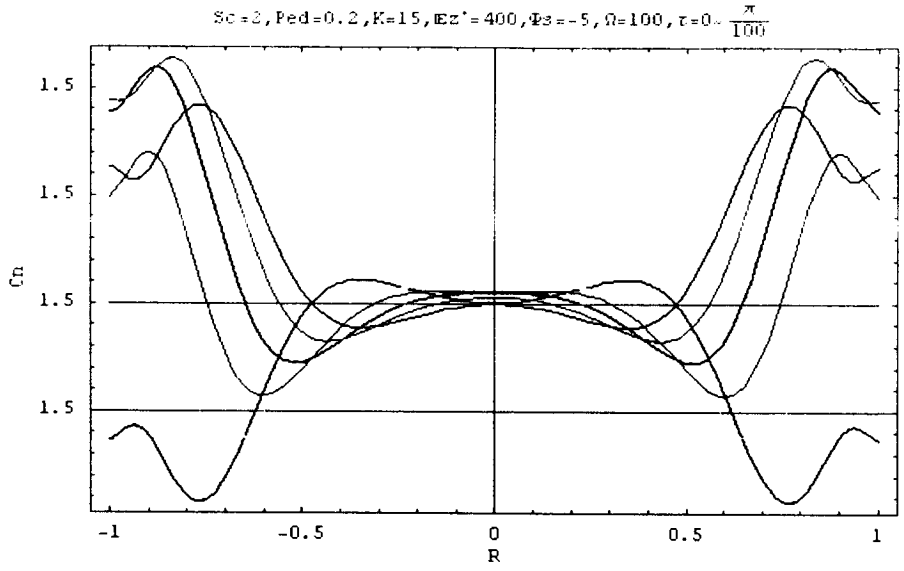

(c)

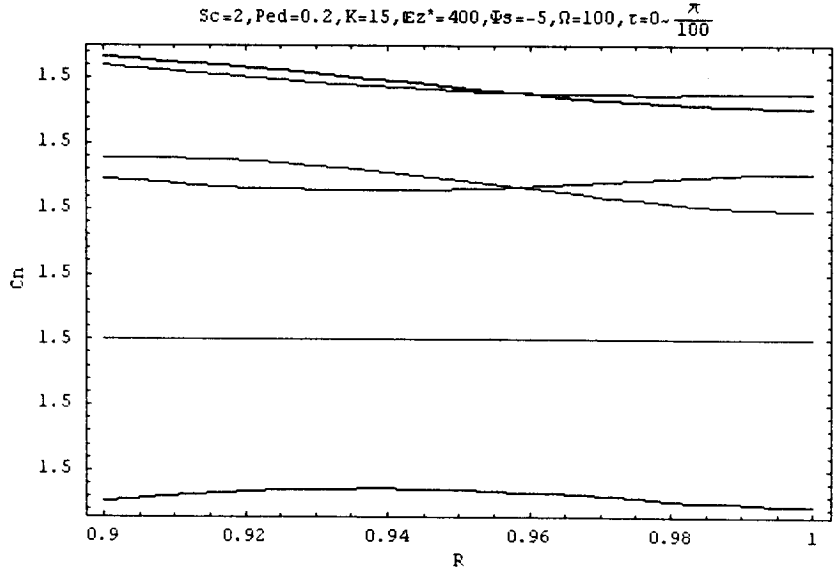

Fig. 4.1-11 (a) The velocity profile, (b) the concentration profile, and (c) the concentration profile between $r = 0.9 \sim 1$ in the microtube at $Z = 500$, $S_c = 2$, $\widetilde{P}_{eD} = 0.2$, $K = 15$, $E_z^* = 400$, and $\Psi_s = -5$, under the dimensionless frequency $\Omega = 100$ during $\Omega\tau = 0 \sim \pi$